

REPORT DOCUMENTATION PAGE
*Form Approved
OMB No. 0704-0188*

The public reporting burden for this collection of information is estimated to average 1 hour per response, including the time for reviewing instructions, searching existing data sources, gathering and maintaining the data needed, and completing and reviewing the collection of information. Send comments regarding this burden estimate or any other aspect of this collection of information, including suggestions for reducing the burden, to the Department of Defense, Executive Services and Communications Directorate (0704-0188). Respondents should be aware that notwithstanding any other provision of law, no person shall be subject to any penalty for failing to comply with a collection of information if it does not display a currently valid OMB control number.

PLEASE DO NOT RETURN YOUR FORM TO THE ABOVE ORGANIZATION.

1. REPORT DATE (DD-MM-YYYY) 31-05-2013	2. REPORT TYPE Journal Article	3. DATES COVERED (From - To)		
4. TITLE AND SUBTITLE Observations on the Characteristics of the Exchange Flow in the Dardanelles Strait		5a. CONTRACT NUMBER		
		5b. GRANT NUMBER		
		5c. PROGRAM ELEMENT NUMBER 061153N		
6. AUTHOR(S) Ewa Jarosz, William J. Teague, Jeffrey W. Book, Sukru T. Besiktepe		5d. PROJECT NUMBER		
		5e. TASK NUMBER		
		5f. WORK UNIT NUMBER 73-9441-02-5		
7. PERFORMING ORGANIZATION NAME(S) AND ADDRESS(ES) Naval Research Laboratory Oceanography Division Stennis Space Center, MS 39529-5004		8. PERFORMING ORGANIZATION REPORT NUMBER NRL/JA/7330--12-1170		
9. SPONSORING/MONITORING AGENCY NAME(S) AND ADDRESS(ES) Office of Naval Research One Liberty Center 875 North Randolph Street, Suite 1425 Arlington, VA 22203-1995		10. SPONSOR/MONITOR'S ACRONYM(S) ONR		
		11. SPONSOR/MONITOR'S REPORT NUMBER(S)		
12. DISTRIBUTION/AVAILABILITY STATEMENT Approved for public release, distribution is unlimited.				
13. SUPPLEMENTARY NOTES				
14. ABSTRACT A mooring section at each end of the Dardanelles Strait was deployed by the Naval Research Laboratory on 28–29 August 2008 and maintained until 11 October 2009. Each section was equipped with two bottom-mounted Barny moorings and a vertical string that together delivered concurrent bottom pressure, temperature, salinity, and almost full-water column current velocity observations. These observations at the mooring sections indicated that on longer timescales (monthly or longer), the exchange through the Dardanelles Strait showed little variability and had a two-layer structure with brackish waters moving approximately southward in the upper layer and more saline Aegean waters flowing roughly northward underneath. On shorter time scales (synoptic), there were pronounced fluctuations in both layers. In the northern section, some manifested as almost simultaneous reversals of the flow direction in both layers with lighter upper-layer waters backing into the Sea of Marmara and dense lower-layer waters moving toward the Aegean Sea. In the southern section, some of the exchange variability consisted of a three-layer flow structure with upper brackish and bottom salty layers moving toward the Aegean Sea and a middle salty layer flowing toward the Sea of Marmara. This three-layer exchange persisted from a day to a week. Synoptic flow variability in the upper layer was partly related to both the along-strait wind stress and the bottom pressure anomaly gradient, while lower-layer current fluctuations were coherent with the bottom pressure anomaly gradient.				
15. SUBJECT TERMS Dardanelles Strait, current variability, exchange flow				
16. SECURITY CLASSIFICATION OF: a. REPORT Unclassified		17. LIMITATION OF ABSTRACT UU	18. NUMBER OF PAGES 18	19a. NAME OF RESPONSIBLE PERSON Ewa Jarosz
b. ABSTRACT Unclassified				19b. TELEPHONE NUMBER (Include area code) (228) 688-4292
c. THIS PAGE Unclassified				

*Standard Form 298 (Rev. 8/98)
Prescribed by ANSI Std. Z39.18*

Observations on the characteristics of the exchange flow in the Dardanelles Strait

Ewa Jarosz,¹ William J. Teague,¹ Jeffrey W. Book,¹ and Şükrü T. Beşiktepe²

Received 10 July 2012; revised 25 September 2012; accepted 26 September 2012; published 9 November 2012.

[1] A mooring section at each end of the Dardanelles Strait was deployed by the Naval Research Laboratory on 28–29 August 2008 and maintained until 11 October 2009. Each section was equipped with two bottom-mounted Barny moorings and a vertical string that together delivered concurrent bottom pressure, temperature, salinity, and almost full-water column current velocity observations. These observations at the mooring sections indicated that on longer timescales (monthly or longer), the exchange through the Dardanelles Strait showed little variability and had a two-layer structure with brackish waters moving approximately southward in the upper layer and more saline Aegean waters flowing roughly northward underneath. On shorter time scales (synoptic), there were pronounced fluctuations in both layers. In the northern section, some manifested as almost simultaneous reversals of the flow direction in both layers with lighter upper-layer waters backing into the Sea of Marmara and dense lower-layer waters moving toward the Aegean Sea. In the southern section, some of the exchange variability consisted of a three-layer flow structure with upper brackish and bottom salty layers moving toward the Aegean Sea and a middle salty layer flowing toward the Sea of Marmara. This three-layer exchange persisted from a day to a week. Synoptic flow variability in the upper layer was partly related to both the along-strait wind stress and the bottom pressure anomaly gradient, while lower-layer current fluctuations were coherent with the bottom pressure anomaly gradient.

Citation: Jarosz, E., W. J. Teague, J. W. Book, and Ş. T. Beşiktepe (2012), Observations on the characteristics of the exchange flow in the Dardanelles Strait, *J. Geophys. Res.*, 117, C11012, doi:10.1029/2012JC008348.

1. Introduction

[2] The Dardanelles Strait (also referred to as the Çanakkale Strait) connects the Sea of Marmara and the Aegean Sea. It is a part of the Turkish Straits System (TSS) that also consists of the Sea of Marmara and the Bosphorus Strait located further north. The Dardanelles Strait is about 61 km long with an averaged depth of 55 m. The strait is rather narrow with a width varying between 1.2 km and 7 km [Ünlüata *et al.*, 1990]. The narrowest section of the Dardanelles Strait is located in a sharp bend called the Nara Pass.

[3] The Dardanelles Strait is a pathway for low-salinity waters originating in the Black Sea to flow into the Aegean Sea. It is also a conduit for high-salinity waters moving from the Aegean Sea to the Sea of Marmara and then to the Black Sea. As a result, the mean exchange flow in this strait has a two-layer structure. This mean two-layer exchange flow is driven by a density difference and modified by a sea elevation difference between the adjacent basins. Density in this

strait is dominated by salinity despite significant seasonal changes in temperature. Historical hydrographic observations show a relatively uniform, thick, brackish upper layer between the Sea of Marmara and a section just north of the Nara Pass [Ünlüata *et al.*, 1990]. Beyond the pass to the Aegean Sea exit, the interface rises and the upper layer becomes thinner and more saline implying enhanced mixing processes in this part of the strait [Ünlüata *et al.*, 1990; Eremeev *et al.*, 1999]. Consequently, large amounts of lower-layer waters, i.e., approximately 43%–45% of the inflow, is entrained in the upper layer and returned back to the Aegean Sea as estimated from the volume and salt flux conservation [see, e.g., Ünlüata *et al.*, 1990; Tuğrul *et al.*, 2002].

[4] A few modeling studies have been done for the Dardanelles Strait over the years. Results from the two-layer model developed by *Oğuz and Sur* [1989] showed asymmetry and rapid transition of the interface depth as well as intense mixing south of the Nara Pass. They also indicated that the upper-layer flow is controlled and that there are two hydraulic controls: one at the Nara Pass and another at an abrupt expansion of the strait width at the Aegean exit, while the lower layer flows subcritically through the strait. *Stashchuk and Hutter* [2001] developed a two-dimensional, nonhydrostatic, nonlinear numerical model. Results from this model indicated that in terms of the Froude number, the upper-layer flow is hydraulically controlled and supercritical only near the Nara Pass, while the lower-layer flow is subcritical throughout

¹Naval Research Laboratory, Stennis Space Center, Mississippi, USA.

²Institute of Marine Sciences and Technology, Dokuz Eylül University, Izmir, Turkey.

Corresponding author: E. Jarosz, Naval Research Laboratory, Code 7332, Stennis Space Center, MS 39529, USA.
(ewa.jarosz@nrlssc.navy.mil)

©2012. American Geophysical Union. All Rights Reserved.
0148-0227/12/2012JC008348

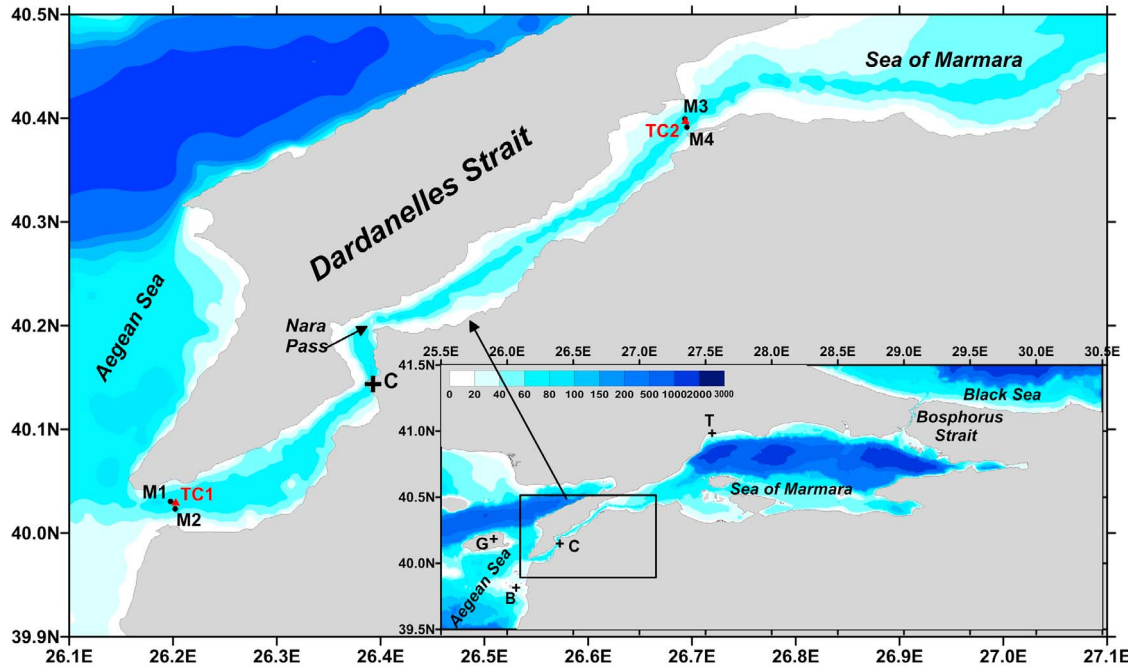


Figure 1. Maps of the Dardanelles Strait and the Turkish Straits System (insert). Moorings and meteorological stations are also shown: Barny moorings (black dots; M1–M4), TC moorings (red triangles, TC1–TC2), and meteorological stations (black pluses; Tekirdağ (T), Çanakkale (C), Gökçeada (G), and Bozcaada (B)). Depth contours are in meters (color bar).

the strait. Somewhat contrary findings came from a three-dimensional numerical model by *Kanarska and Maderich* [2003]. Their simulations showed that there is no hydraulic control near the Nara Pass in summer. *Kanarska and Maderich* [2008] continued their investigation of Dardanelles dynamics by considering mechanisms governing the exchange on a seasonal scale. They found that the seasonal exchange dynamics are governed by turbulent friction and entrainment in the vicinity of the Nara Pass. Their results also indicated that there is weak seasonal variability of the upper-layer flux to the Aegean Sea. In contrast, they found significant seasonal variability in the lower-layer water flux reaching the Sea of Marmara. Additionally, the composite two-layer Froude number estimated from their model data is significantly lower than 1 along the entire strait. In terms of the three-layer hydraulic theory; however, the exchange flow was partially controlled in the Nara Pass region.

[5] In this paper, recent and unique concurrent observations of current, temperature, salinity, bottom pressure, wind, and atmospheric pressure over a yearlong period are analyzed to investigate flow variability in detail in the northern and southern Dardanelles Strait and the impact of atmospheric forcing and bottom pressure anomaly gradient on this exchange flow. Volume fluxes will be the subject of another manuscript. This paper is organized as follows: section 2 describes the deployment, instrumentation, and measurements. Atmospheric forcing, bottom pressure, and stratification in the northern and southern Dardanelles Strait are described in section 3. In section 4, flow variability is analyzed at the mooring locations. Impacts of the forcings on the exchange flow are discussed in section 5. The possibility of hydraulic control in the southern Dardanelles Strait is

considered in section 6. Finally, findings are summarized in section 7.

2. Instrumentation and Observations

[6] The United States Naval Research Laboratory (NRL) and the North Atlantic Treaty Organization (NATO) Undersea Research Center (NURC) in collaboration with the Turkish Navy Office of Navigation, Hydrography, and Oceanography deployed two mooring sections in the Dardanelles Strait at the Aegean and Sea of Marmara entrances. The instruments were deployed from the R/V Alliance (a NATO NURC research vessel) as a part of TSS08 (NURC project) and “Exchange Processes in Ocean Straits” (EPOS, NRL project) programs at the end of August 2008 (Figure 1 and Table 1). Each section was configured with two Barny moorings (called a “Barny” since it shape resembles a barnacle [*Perkins et al.*, 2000]) and one line mooring (Temperature/Conductivity (TC) mooring). At each end of the strait, a Barny mooring and a TC line mooring were deployed in the deep channel, and another Barny mooring was deployed nearby in the eastern side of the shallower part of the channel. Each trawl-resistant bottom-mounted Barny mooring contained the following instrumentation: an upward looking 300-kHz ADCP, a wave/tide gauge (Sea-Bird Electronics 26), and a conductivity (Sea-Bird Electronics 4) sensor. The ADCP heads were set about 0.5 m above the bottom. Current profiles were recorded at 1-m vertical resolution every 15 min. Line moorings (TC moorings) were equipped with seven temperature, conductivity, and pressure sensors. These sensors were Sea-Bird Electronics MicroCATs 37 and In Situ Aqua Trolls, and they recorded data at 15-min intervals. All moorings were serviced and

Table 1. Mooring Summary

Mooring	Latitude	Longitude	Water Depth (m)	Start Time	Stop Time	Depth Range ^a or Instrument Depth ^b (m)
<i>BARNY Moorings</i>						
M1	40° 01.832'	26°11.854'	96.2	08/28/2008	02/07/2009	7.1–92.1
	40° 01.838'	26°11.898'	96.8	02/18/2009	10/11/2009	
<i>T/C Moorings</i>						
TC1: AT11 ^{c,e}	40° 01.811'	26°12.155'	99	08/28/2008	02/07/2009	97.0
MC12 ^d						73.7
MC13						52.1
AT14 ^e						42.5
MC15						37.4
MC16						32.4
MC17						27.3
TC1: AT11 ^f	40° 01.801'	26°12.182'	99	12/18/2009	10/11/2009	97.0
MC12						74.0
MC13						52.0
MC14						42.1
MC15						37.1
MC16						32.1
MC17						27.0
TC2: AT21 ^e	40° 23.877'	26°41.627'	76	08/29/2008	02/07/2009	72.7
MC22 ^f						62.5
MC23						39.1
AT24 ^e						30.6
MC25 ^f						25.5
MC26						20.8
MC27						16.0
TC2: AT21 ^f	40° 23.909'	26°41.676'	75	02/17/2009	10/11/2009	73.0
MC22						68.8
MC23						48.8
MC24						37.5
MC25 ^f						32.2
MC26						28.6
MC27						24.9

^aDepth range is the depth range over which data were collected at each ADCP instrument (M1–M4).

^bInstrument depth is the depth below the surface of Aqua Troll and MicroCAT instruments.

^cAT is Aqua Troll instruments.

^dMC is MicroCAT instruments.

^eAT11, AT14, AT21, and AT24, no conductivity data during the first deployment period.

^fAT11, AT21, MC22, and MC25, some conductivity data during the second deployment period.

redeployed approximately at the same locations in February 2009. The final recovery occurred in October 2009.

[7] Full time series of data were returned from the Barny moorings. Unfortunately, data from the TC moorings were incomplete because five of the sensors failed and returned partial time series of conductivity or none at all. Because locations of the moorings for both deployments were almost identical, observations were combined into single time series for all analyses. Additionally, ADCP observations from both deployments were interpolated to common depth levels at 1-m vertical resolution. Table 1 lists mooring positions, recording periods, water depths, instruments depths for the TC sensors,

and depth ranges for the ADCP instruments. For the majority of the analyses here, high-frequency fluctuations were also eliminated from the observations by applying a low-pass filter with a 40-h cutoff frequency. Additionally, currents were rotated 10° and 50° counterclockwise from east for the Aegean (southern Dardanelles) and Marmara (northern Dardanelles) sections, respectively, to align with along- and across-strait coordinate axes. Positive along-strait (*u*) values are approximately directed eastward along the Aegean section and northeastward along the Marmara section, while negative values are directed westward along the Aegean section and approximately southwestward along the Marmara section. For

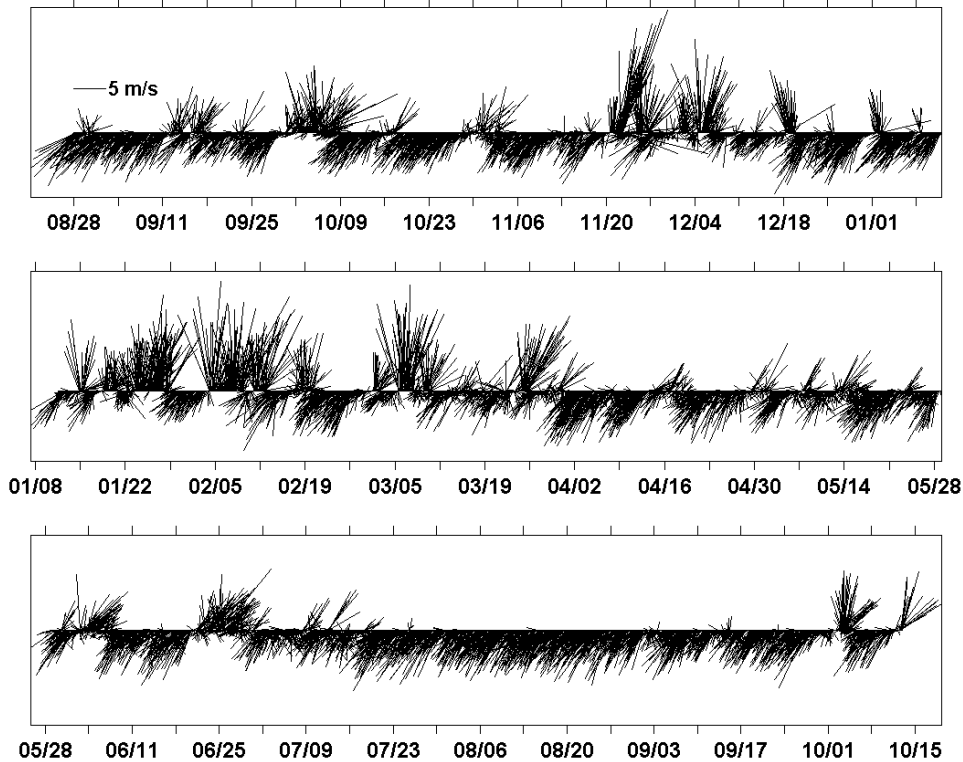


Figure 2. Time series of winds recorded at Çanakkale. Positive x and y axis values indicate winds directed toward the east and the north, respectively. The x axis indicates months and days beginning in 2008.

the across-strait components (v), positive values are toward the European coast, while negative values are toward the Anatolian (Asian) coast.

[8] Concurrent meteorological observations collected at Turkish land stations located inside and near the Dardanelles Strait were also analyzed. Data from the following stations were used: Tekirdağ (T), Çanakkale (C), Gökçeada (G), and Bozcaada (B). The station locations are shown in Figure 1. The analyzed data consisted of hourly measurements of atmospheric pressure, air temperature, wind speed, and wind direction.

3. Exchange Flow Forcing Mechanisms

3.1. Atmospheric Forcing

[9] Prevailing winds over the Dardanelles Strait were mainly northerly to northeasterly (toward south to southwest) during the deployment period. They were disrupted by passages of numerous cyclones that were more common in fall, winter, and early spring as indicated by winds from Çanakkale shown in Figure 2 (winds were plotted using the oceanographic convention with positive values indicating wind components directed toward north and east). Northeasterlies were characterized by lower wind speed, usually below 10 m/s. Higher wind speeds were primarily associated with cyclones that often brought sustained winds over 15 m/s. The most energetic cyclone with winds over 20 m/s impacted the Dardanelles Strait on 21 November 2008 and lasted for about 3 days. The TSS region is generally highly impacted by cyclones between October and April, while winds from the

northward quadrant, which are also called Etesian winds, are dominant between May and September [Ünliata *et al.*, 1990]. Hence the winds from Çanakkale (Figure 2) recorded during the deployment seem very typical for this region. Winds recorded at Bozcaada (not shown), an island station, were generally similar to those recorded at Çanakkale, while winds at Gökçeada, another island station, seemed to be characterized by slightly lower speeds but very similar wind directions to those observed at Çanakkale and Bozcaada.

[10] The atmospheric pressure field was very homogeneous over the region (Figure 3a). Fluctuations among all four locations were very coherent and in phase for frequencies less than 0.6 cycle per day (cpd). This homogeneity of the atmospheric pressure field resulted in a rather small horizontal gradient of atmospheric pressure across the Dardanelles Strait (magnitudes less than 10^{-6} kPa/m; Figure 3b).

3.2. Bottom Pressure Anomalies

[11] Bottom pressure measurements collected at the Barny moorings allowed an evaluation of pressure variations along the Marmara and Aegean sections. Specifically, the measured bottom pressure variation can be broken into components as follows:

$$p'_b = p'_{Atm} + \rho_0 g \eta' + g \int_{-H}^0 \rho' dz \quad (1)$$

where p'_{Atm} is the atmospheric pressure, η' is the water level, ρ' is the density, g is gravitational acceleration, ρ_0 is the reference density, and H is the total depth. The primes

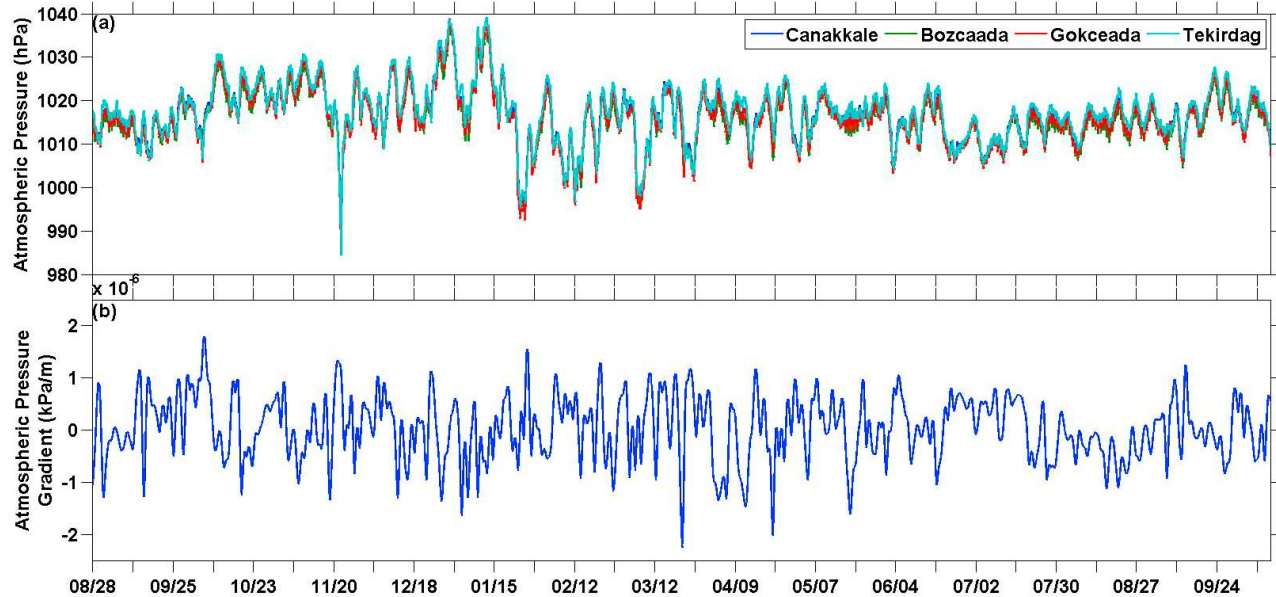


Figure 3. (a) Times series of atmospheric pressure from Çanakkale, Bozcaada, Gökçeada, and Tekirdağ and (b) time series of the atmospheric pressure gradient estimated from observations (40-h low-passed data) collected at Bozcaada and Tekirdağ.

indicate that the time means were removed, and all pressure and pressure differences discussed hereafter are from such pressure anomalies. Figure 4 displays the time series of the 40-h low-passed bottom pressure anomalies at each location and the time series of the bottom pressure anomaly differences (BPD) between the southern and northern Dardanelles Strait and along each section. The BPD is considered here as

a potential forcing of observed exchange flow variations. Fluctuations of the bottom pressure were almost identical, very coherent, and in phase for the mooring sites located at the same section (for both sections, coherence squared is larger than 0.97 for frequencies less than 0.6 cpd). Along the Marmara section the bottom pressure anomalies varied between -2.2 kPa and 2.3 kPa , while the concurrent bottom

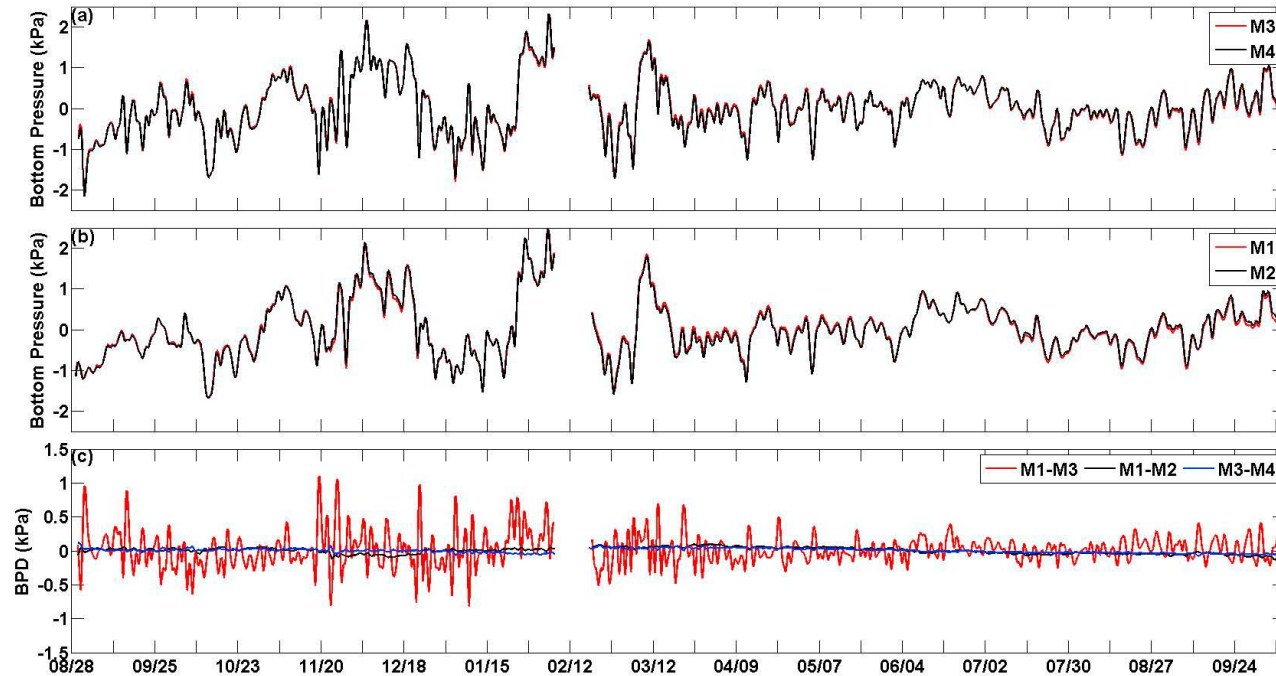


Figure 4. Bottom pressure (kPa; 40-h low-passed data) in the (a) northern (moorings M3 and M4) and (b) southern Dardanelles Strait (moorings M1 and M2), and (c) bottom pressure anomaly differences (BPD) between M1 and M3, M1 and M2, M3 and M4 (kPa).

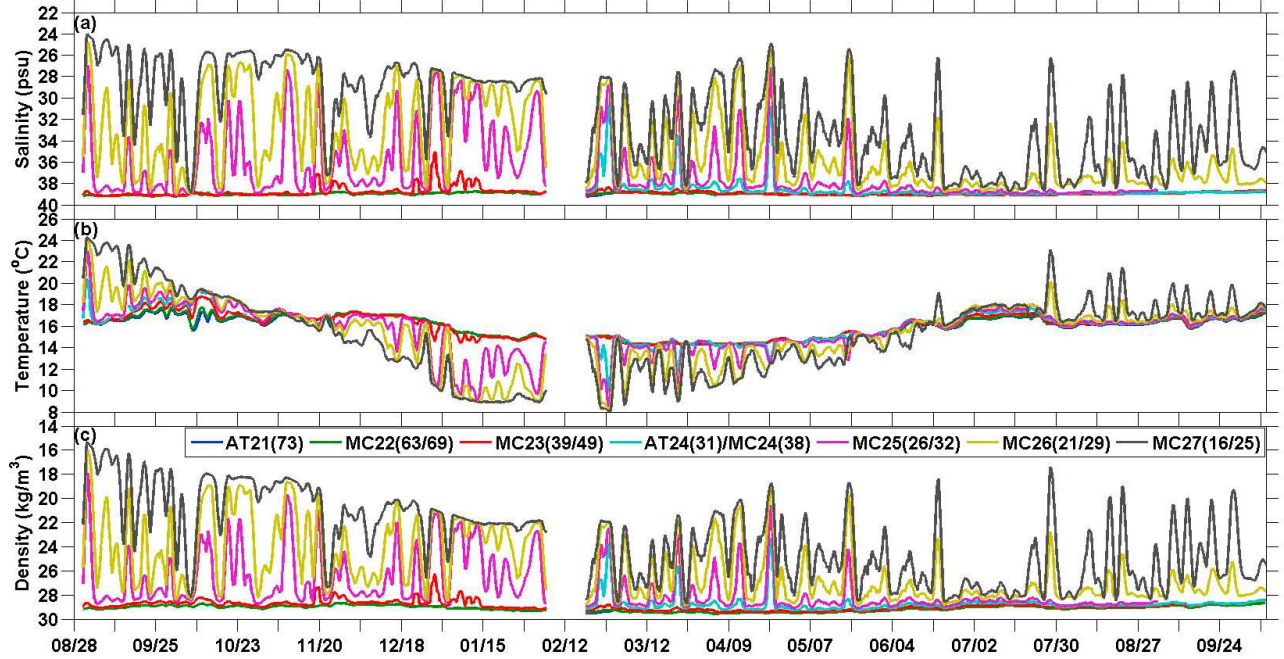


Figure 5. (a) Salinity, (b) temperature, and (c) density in the northern Dardanelles Strait (40-h low-passed data). Instrument types and numbers with their depths in meters in parenthesis are also given.

pressure anomalies fluctuated between -1.7 kPa and 2.5 kPa along the Aegean section. The bottom pressure fluctuations were similar between the two sections, and consequently, the BPD did not reach high values and was between -0.8 kPa and 1.1 kPa (Figure 4c). There were also some differences in the bottom pressure anomalies between these two mooring sections, especially for higher-frequency fluctuations that resulted in coherence squared decreasing almost linearly with increasing frequencies from 0.92 at 0.1 cpd to 0.11 at 0.6 cpd indicating that BPD variability was more pronounced over shorter timescales.

3.3. Stratification

[12] Figure 5 shows salinity, temperature, and density (σ_0) recorded in the northern Dardanelles Strait (TC2; 40-h low-passed data). The lowest recorded salinity at this section was 24.05 psu (16 m). Low salinity waters (less than 30 psu) often extended as deep as 26 m to 32 m below the surface. A thicker upper layer (over 26 m) was commonly observed during the winter and spring while in summer and fall, the upper layer was generally only about 20-m thick (also indicated by the currents shown in Figure 7). This change in thickness coupled with instrument placements (Table 1) caused the upper layer to be better resolved during the first part of the deployment than during the second part. During moderate to strong northeasterly winds blowing over the region, the upper layer usually expanded and on occasion, salinities less than 30 psu were recorded as deep as 32 m. When the northeasterly winds weakened or if a storm with strong winds passed over the TSS region then the upper layer usually contracted, and due to vigorous mixing, salinity as high as 38 psu was recorded by the 20-m sensor and even by the 16-m sensor on occasion. The lower-layer salinity varied little over the observational period, especially below 50 m. The mean salinity estimated from the

observations was 38.87 psu in this layer. Temperature in the upper layer clearly reflected seasonal changes and was as high as 24.31°C in summer and dropped as low as 8.02°C in winter. The lower layer had much less thermal variability with temperature varying between 14.25°C and 17.73°C .

[13] Salinity, temperature, and density from the southern Dardanelles Strait (TC1; 40-h low-passed data) are shown in Figure 6. Unfortunately, the TC1 mooring did not have any sensors in the upper layer; thus salinity variability in this layer cannot be discussed here. The observations, however, resolved the lower layer well. The salinity varied little there and on average, it was 39.09 psu. Lower salinity (less than 38 psu) was generally measured only by the shallowest sensor (27 m) and these low values were usually associated with passing storms and accompanying mixing. Also note that salinity dropped below 38 psu even at 32 m on one occasion when strong winds associated with a cyclone moving over the TSS were able to generate strong mixing. For this section as well as for the northern section, density was more a function of salinity rather than of temperature (Figures 5c and 6c). Temperature in the lower layer displayed more variability at the Aegean section and varied between 13.13°C and 19.59°C . Larger temperature ranges (over 4.5°C) were recorded at depths of 37 m and shallower, and this larger variability can be attributed to the proximity to the surface and reflects seasonal heating and cooling changes.

4. Exchange Flow

4.1. Mean Flow and Its Seasonality

[14] Record-long averages of the current velocities clearly demonstrated that at the mooring sections, the mean exchange in the Dardanelles Strait had a well-defined two-

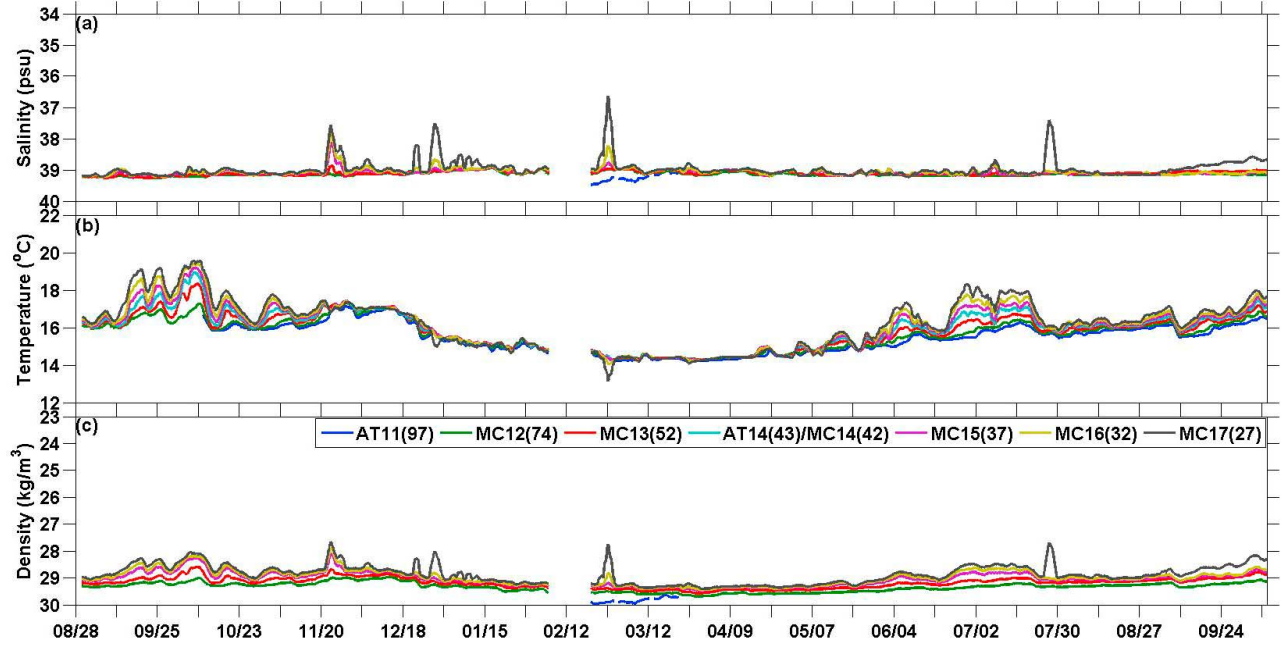


Figure 6. (a) Salinity, (b) temperature, and (c) density in the southern Dardanelles Strait (40-h low-passed data). Instrument types and numbers with their depths in meters in parenthesis are also given.

layer structure at both ends (Table 2 and Figures 7a and 8a). It is also apparent that the mean thickness of the upper layer decreases from the Marmara end to the Aegean end. It was, on average, about 22 m thick near the Sea of Marmara and

about 13 m thick near the Aegean Sea as indicated by a 0 along-strait velocity crossing. The mean along-strait currents in the upper layer had speeds of about 40 cm/s and over 70 cm/s in the northern and southern Dardanelles,

Table 2. Current Statistics^a

Mooring/Depth (m)	u_{mean} (cm/s)	u_{std} (cm/s)	$u_{\text{err}}^{\text{b}}$ (cm/s)	u_{max} (cm/s)	u_{min} (cm/s)	v_{mean} (cm/s)	v_{std} (cm/s)	$v_{\text{err}}^{\text{b}}$ (cm/s)	v_{max} (cm/s)	v_{min} (cm/s)
M1/7.1	-53.9	26.4	5.1	74.7	-109.5	-3.7	6.5	0.5	15.4	-21.9
M1/10.1	-27.5	25.2	4.8	79.1	-91.1	4.9	5.9	0.6	20.3	-13.8
M1/13.1	-2.5	24.5	5.8	76.6	-73.3	6.9	6.4	0.8	33.0	-11.3
M1/16.1	13.0	21.4	7.5	71.8	-60.3	4.8	6.6	0.6	44.8	-10.1
M1/24.1	20.0	13.0	3.9	62.6	-31.3	-0.7	2.9	0.2	20.8	-9.2
M1/40.1	15.2	9.8	0.7	42.9	-20.6	-2.7	2.4	0.6	6.5	-10.5
M1/60.1	10.1	10.4	0.7	47.1	-20.4	-2.0	2.0	0.2	3.3	-8.5
M1/90.1	4.3	9.8	0.7	47.5	-14.6	-1.1	1.7	0.1	5.2	-10.0
M2/5.3	-68.4	27.5	5.5	88.0	-130.5	-9.5	7.1	1.8	11.2	-29.7
M2/8.3	-45.3	27.4	5.3	85.0	-107.0	3.5	7.3	1.4	23.5	-20.2
M2/12.3	-4.1	29.7	6.9	82.5	-83.7	7.4	7.3	0.6	33.2	-12.3
M2/16.3	19.9	22.0	8.6	73.7	-64.6	3.0	6.6	1.1	46.5	-12.4
M2/24.3	26.2	10.3	3.1	61.2	-23.9	-1.3	3.3	0.7	24.0	-12.1
M2/40.3	20.5	8.7	0.5	64.1	-7.6	-2.7	2.3	0.6	3.9	-11.8
M2/60.3	13.6	9.4	0.7	55.5	-13.2	-0.3	2.2	0.6	7.8	-7.3
M3/5.7	-40.7	21.7	1.3	113.0	-103.4	5.8	3.7	0.2	19.8	-8.9
M3/10.7	-39.0	20.8	1.2	83.6	-123.7	6.8	3.7	0.3	19.8	-6.7
M3/21.7	-1.3	22.2	8.9	53.7	-74.8	3.7	3.9	1.3	20.9	-8.8
M3/30.7	20.7	19.0	4.6	71.9	-50.1	3.5	2.7	0.1	13.0	-4.8
M3/40.7	24.1	15.7	0.9	82.2	-39.5	2.1	2.0	0.3	14.6	-2.1
M3/55.7	20.6	13.0	0.7	70.2	-29.7	-0.5	1.4	0.3	4.4	-4.6
M3/65.7	16.2	11.0	0.6	58.3	-23.1	-1.4	1.4	0.1	3.1	-6.4
M4/5.0	-40.3	22.2	1.3	122.3	-121.4	8.6	4.5	1.9	23.9	-6.1
M4/10.0	-38.4	20.7	1.1	91.0	-123.9	8.7	4.3	0.3	24.1	-5.0
M4/21.0	-0.7	17.3	7.5	46.6	-65.6	4.7	3.5	1.0	18.9	-3.6
M4/30.0	15.5	14.4	3.4	51.4	-50.8	6.5	3.3	0.2	25.5	-2.1
M4/40.0	18.2	12.7	0.8	62.4	-32.2	6.5	3.5	0.2	23.2	-3.2
M4/55.0	16.0	11.1	0.6	57.4	-25.5	6.1	3.6	0.2	23.6	-3.2
M4/63.0	13.6	9.6	0.5	46.6	-24.5	6.2	4.2	0.2	25.3	-6.0

^aMeans (u_{mean} , v_{mean}), standard deviations (u_{std} , v_{std}), root-mean square errors of velocity means (u_{err} , v_{err}), maximum (u_{max} , v_{max}), and minimum (u_{min} , v_{min}) values of the along- (u) and across-strait (v) velocity components.

^bRoot-mean square errors are defined as the standard deviation divided by the squared root of the degrees of freedom; the degrees of freedom were estimated as the sampling period divided by the integral timescale.

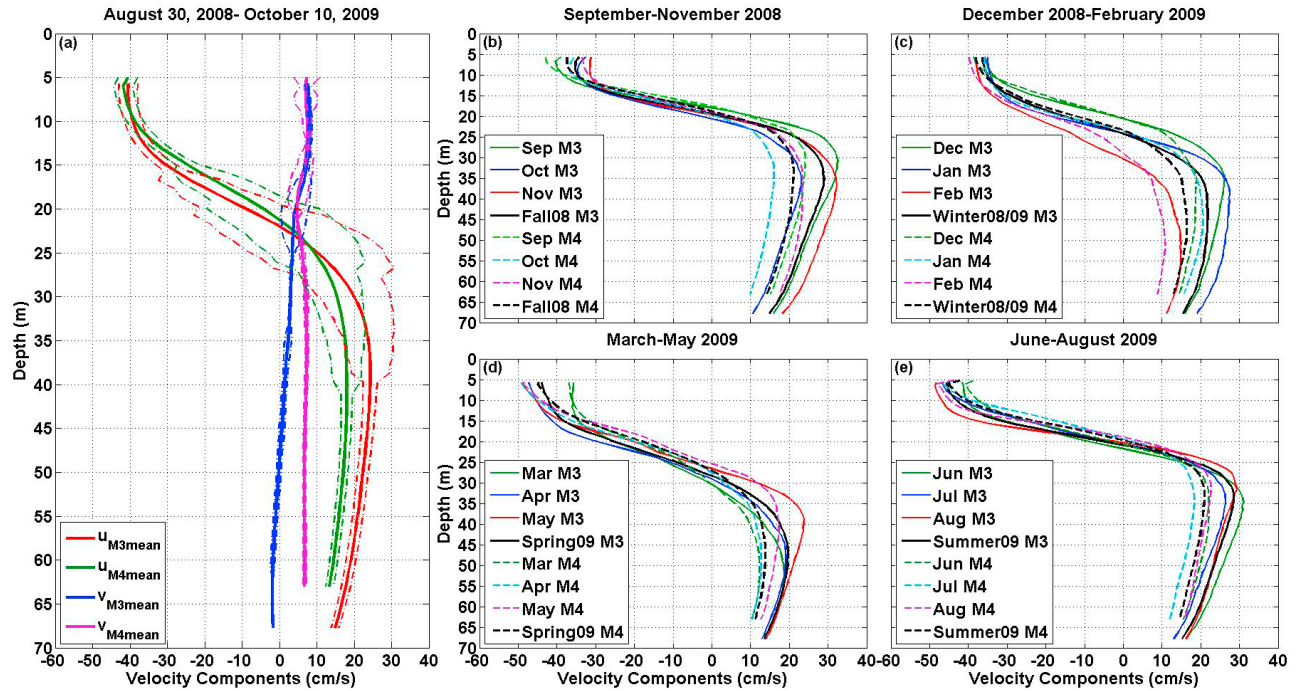


Figure 7. (a) Profiles of the record means at the Marmara section (along-strait current components: M3, red line, M4, green line; across-strait current components: M3, blue lines, M4, magenta line) and 95% confidence intervals of the respective means (dash-dotted lines); (b–e) monthly and seasonal means of the along-strait current components (M3, colored solid lines, M4, colored dashed lines).

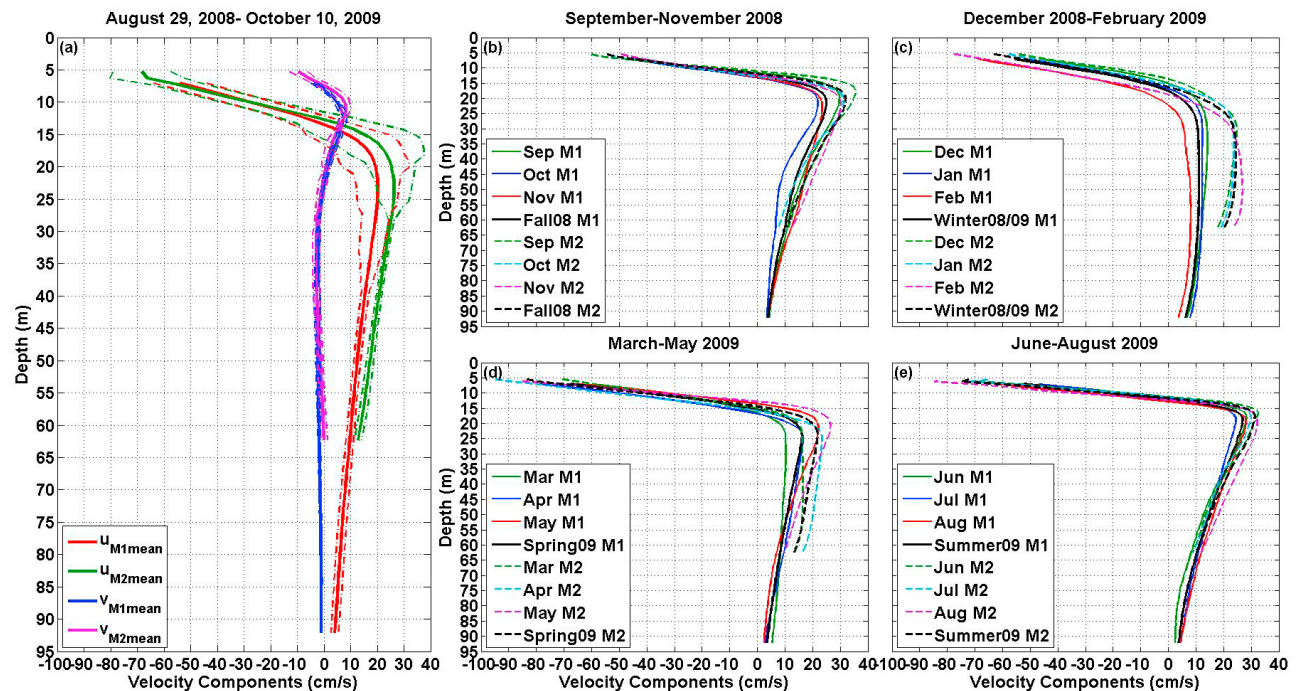


Figure 8. (a) Profiles of the record means at the Aegean section (along-strait current components: M1, red line, M2, green line; across-strait current components: M1, blue lines, M2, magenta line) and 95% confidence intervals of the respective means (dash-dotted lines); (b–e) monthly and seasonal means of the along-strait current components (M1, colored solid lines, M2, colored dashed lines).

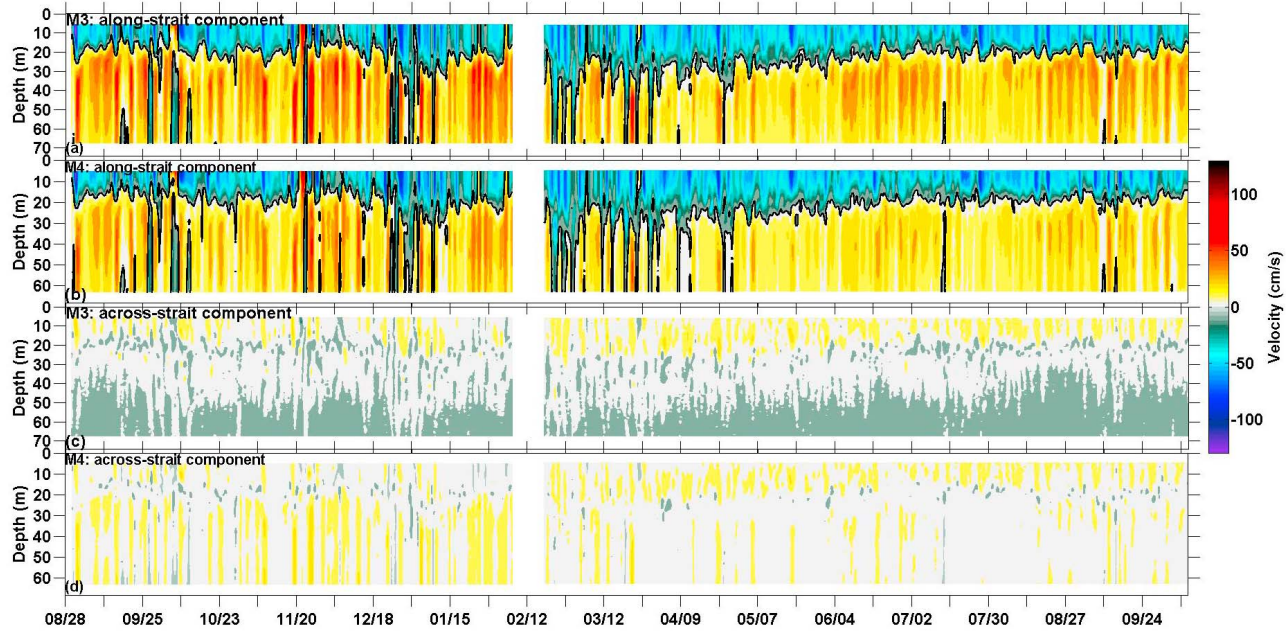


Figure 9. Currents in the northern Dardanelles (40-h low-passed data): along-strait current components at (a) M3 and (b) M4, and across-strait current component at (c) M3 and (d) M4. A 0-velocity isotach is drawn by a black line in Figures 9a and 9b.

respectively. The lower layer was much thicker than the upper layer, i.e., more than 40 m and 80 m in the northern and southern sections, respectively, and mean currents were weaker than those of the upper layer. Mean currents for the lower layer were up to 24 cm/s and 26 cm/s at the northern and southern Dardanelles, respectively. Table 2 provides a summary of current statistics from the moorings.

[15] The two-layer flow structure was also confirmed by seasonal and monthly averages (Figures 7b–7e and Figures 8b–8e). These data also indicate the existence of monthly and seasonal variability in flow speeds and layer thicknesses. At the northern section, the upper-layer flow reached a high of about 50 cm/s in late spring and summer 2009, while the flow in the lower layer had higher mean values in fall 2008 and late summer 2009. As indicated also by salinity (Figure 5a), the upper layer began deepening in January 2009 and thickened to 25–30 m between February and May 2009 (Figures 7b–7e). During the remaining part of the deployment, the thickness of this layer was generally about 22 m. In the southern Dardanelles, currents in the upper layer were strongest (>70 cm/s) in spring 2009. Higher mean velocities (>30 cm/s) in the lower layer were observed in fall 2008 and summer 2009 with the speed maximum located about 5 m below the 0 velocity isotach. Additionally, the lower-layer flow was asymmetrical, i.e., the currents were stronger at M2 than those at M1. The upper layer also became thicker in February 2009 and remained about 17 m thick until April 2009.

4.2. Flow Variability

[16] There was great variability around long-term current means in both layers at each location as shown in Figures 9 and 10. It is also apparent that the along-strait velocity component was more energetic than the across-strait velocity component as expected in ocean straits. In the northern Dardanelles, upper-layer along-strait currents often exceeded

80 cm/s, while the flow in the lower layer was usually below 50 cm/s; however, between September 2008 and March 2009, lower-layer currents surpassed 60 cm/s more often. The upper-layer flow was blocked and/or reversed several times. These events were more common between September 2008 and March 2009, and they lasted from several hours as on 5 March 2009 to a few days as between 4 and 7 October 2008. There were also blockages and reversals of the lower-layer flow along the Marmara section. They mainly occurred again between September 2008 and March 2009 and usually lasted from several hours to about 2 days. The longest event occurred between 5 and 8 October 2008 about half a day after the upper-layer flow reversed.

[17] In the southern Dardanelles, the along-strait upper-layer currents were stronger than in the northern Dardanelles and often over 90 cm/s. The maximum recorded flow was 130 cm/s. The lower-layer flow was weaker with a maximum speed of 40 cm/s but generally current speeds there were about 30 cm/s. On shorter timescales, the vertical structure of the exchange flow was more complex at the southern section than at the northern section. The exchange often had a three-layer structure with currents in a third deep layer flowing toward the Aegean Sea with speeds as high as 10 cm/s (Figures 10a and 10b). The three-layer structure prevailed along this section with durations from a day to a week.

4.3. Exchange Flow Asymmetry

[18] The lower-layer flow was clearly asymmetric, i.e., it was stronger at mooring M2 than mooring M1 in the southern Dardanelles Strait (Figures 8 and 10). This intensification was rather unexpected because mooring M2 was deployed in the shallower part of the narrow strait (width (W) \sim 5 km) close to the Anatolian (Asian) coast and currents there should have been reduced at least somewhat by wall/bottom friction. Much stronger currents carrying Aegean

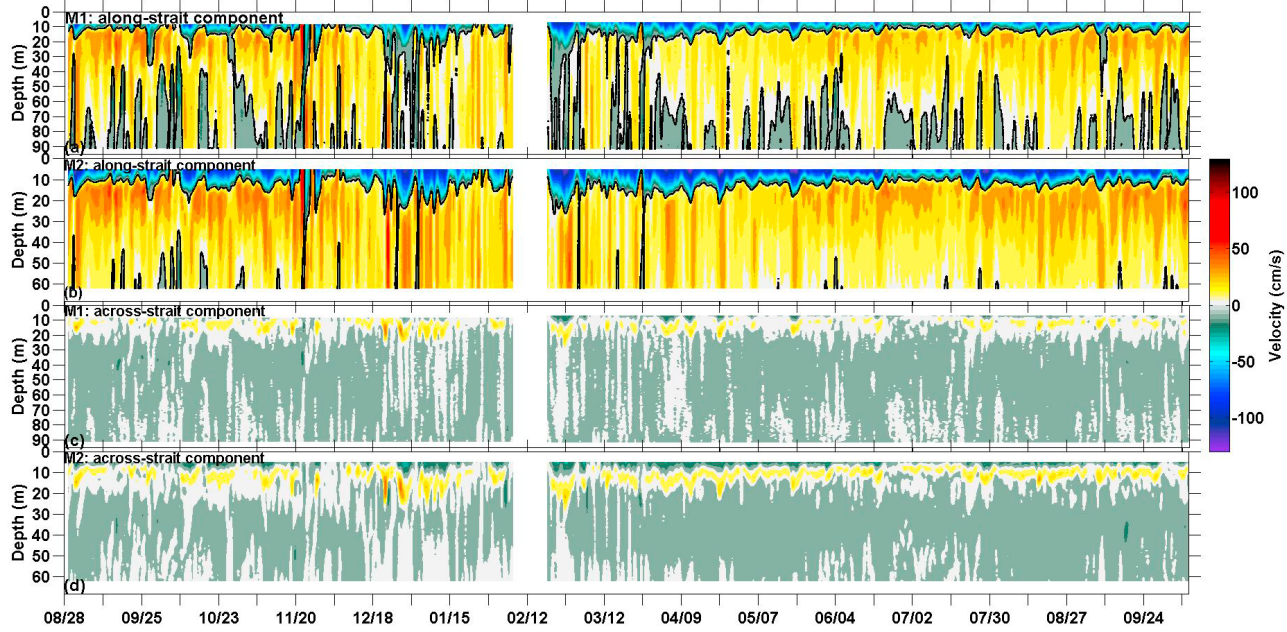


Figure 10. Currents in the southern Dardanelles (40-h low-passed data): along-strait current components at (a) M1 and (b) M2, and across-strait current components at (c) M1 and (d) M2. A 0-velocity isotach is drawn by a black line in Figures 10a and 10b.

waters at M2 were commonly observed between October 2008 and April 2009 and in October 2009. During this time period, mean speed differences between M2 and M1 in the lower layer were from 4 cm/s to 9 cm/s for depths between 15 m and 62 m. The largest measured speed differences were generally found below 20 m where they often were over 15 cm/s. There were only 29 out of 200 days (14.5%) when current speeds were comparable at both moorings. For the remaining part of the deployment, intensification at mooring M2 occurred slightly less frequently (81% days) and it was generally confined to depths between 13 m and 18 m with a mean speed difference of about 8 cm/s. Current speed differences below 19 m were also smaller and usually less than 5 cm/s.

[19] Horizontal flow asymmetry often occurs in density-induced exchange flows in estuaries. It was observed, for example, in the entrance to Chesapeake Bay or the James River estuary [Valle-Levinson *et al.*, 2003]. It was pointed out by Kasai *et al.* [2000] that the water depth, rather than basin's width, should determine whether the Earth's rotation (Coriolis) effects are important for regions of freshwater influence. They argue that Coriolis effects are important regardless of a width of a basin if the water depth (H) is much greater than several Ekman layers ($D_E = (2A_z/f)^{1/2}$, where f is the Coriolis parameter and A_z is the vertical eddy viscosity). In the southern Dardanelles Strait, the water depth is 100 m and the Ekman layer is about 15 m for a representative eddy viscosity of $0.01 \text{ m}^2/\text{s}$. Hence H is about seven times greater than D_E at this location. An eddy viscosity of $0.01 \text{ m}^2/\text{s}$ was chosen to represent average viscosity estimated from microstructure observations collected near this mooring section for the EPOS project.

[20] Valle-Levinson [2008] further investigated impacts of the basin width, friction, and the Earth's rotation on density-induced exchange flows as a function of the Ekman (E_k) and

Kelvin (K_e) numbers. The Ekman number ($E_k = A_z/fH^2$) compares frictional to Coriolis effects, while the Kelvin number ($K_e = W/R_i$) compares the basin width to rotation effects. Rotation effects are important for small E_k and large K_e . R_i is the internal Rossby radius that is given by $(g'h)^{1/2}/f$, where h is the depth of the buoyant part of the density-induced flow and g' is the reduced gravity. The reduced gravity is equal to $g\Delta\rho/\rho_o$, where g is the gravity acceleration, ρ_o is the reference density, and $\Delta\rho$ is the density difference between the layers.

[21] With $g' = 0.057 \text{ m/s}^2$, $h = 13 \text{ m}$, $f = 9.4 \cdot 10^{-5} \text{ s}^{-1}$, and $R_i = 9.1 \text{ km}$, K_e is 0.55, and E_k is 0.01 in the Aegean section, while they are 0.22 and 0.02, respectively, in the Marmara section ($W = 3.5 \text{ km}$, $A_z = 0.01 \text{ m}^2/\text{s}$, $g' = 0.1 \text{ m/s}^2$, $h = 22 \text{ m}$, $f = 9.4 \cdot 10^{-5} \text{ s}^{-1}$, and $R_i = 16 \text{ km}$). Valle-Levinson [2008] concluded that under moderate friction conditions ($0.01 < E_k < 0.1$), the exchange flow is asymmetric, e.g., both horizontally and vertically sheared for most basin widths. This finding may explain asymmetry of the flow in the lower layer along the southern section of the strait ($K_e = 0.55$; see Figure 4d in Valle-Levinson [2008] for a possible configuration of the exchange flow in the southern Dardanelles Strait). Current observations were not collected near the European coast in the southern Dardanelles Strait and current observations from mooring M1 did not resolve near surface currents well enough to prove that there was also asymmetry in the upper-layer flow that would be expected based on the same finding by Valle-Levinson [2008]. There is, however, an indication that this may indeed be the case because the upper layer (depth of the 0-velocity isotach) seemed to be consistently thicker (about 1 m thicker) at mooring M1 than that at mooring M2. In very narrow systems ($K_e < 0.25$) there is no horizontal asymmetry in the exchange flow [Valle-Levinson, 2008] which may help

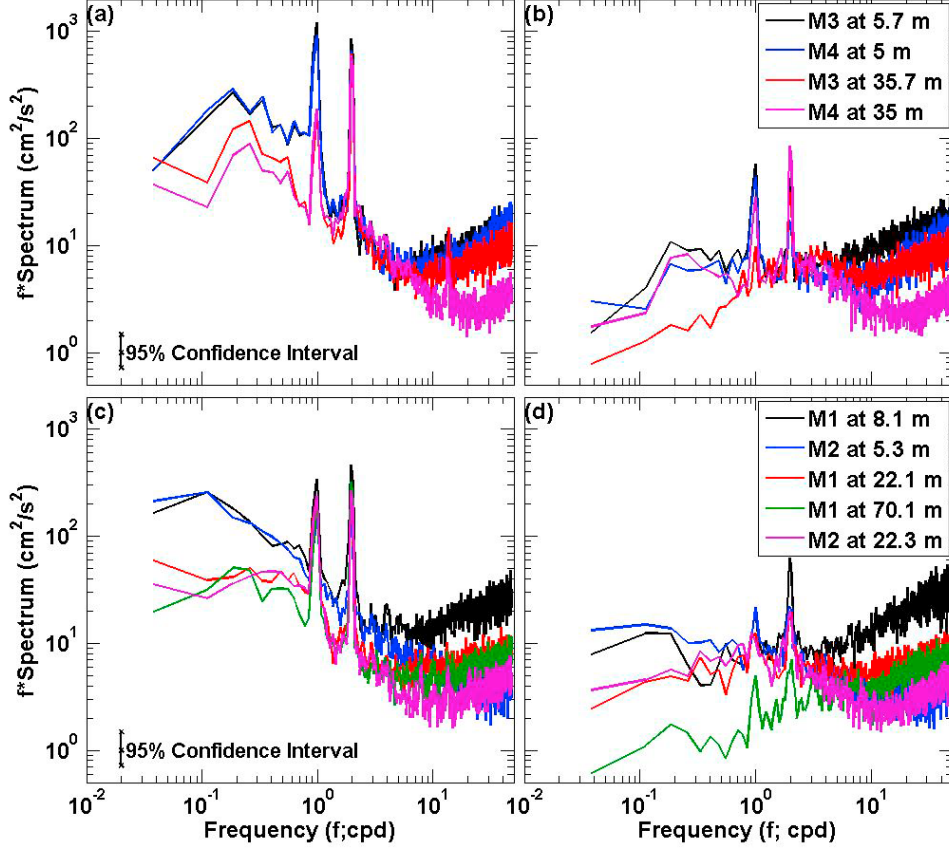


Figure 11. Variance preserving spectra for (a, c) along- and (b, d) across-strait current components at the Marmara section (Figures 11a and 11b) and the Aegean section (Figures 11c and 11d); frequencies in cycles per day (cpd).

to explain the flow structure in the northern Dardanelles Strait where K_e is about 0.22.

4.4. Spectral Characteristics

[22] Variance-preserving current spectra of the along- and across-strait velocity components for a few depths are shown in Figure 11. At both locations and layers, the along-strait velocities were more energetic than the across-strait velocity components for frequencies less than 0.6 cpd. At both mooring sections, there were well-defined peaks at diurnal (~ 1 cpd) and semidiurnal (~ 2 cpd) tidal frequencies and general enhancement in energy at lower frequencies, i.e., at frequencies less than 0.6 cpd. Additionally, the current energy level was higher in the upper layer than that in the lower layer in both the Aegean and Marmara sections.

[23] In the northern and southern Dardanelles, flows at the same depth level but at different mooring locations along the same section were highly coherent as indicated by high values of the coherence squared shown in Figure 12 (black and red lines). In the northern Dardanelles, flows in the upper and lower layers were generally decoupled as implied by low coherence values, except for frequencies near 0.2 cpd (5 days) where the coherence exceeded 0.5. This higher value seems to indicate that 5-day current fluctuations were fairly common in both layers and, under certain conditions, the flows were coupled in the northern section. In the southern Dardanelles, current relationships in the lower layer

were more complex, especially at mooring M1. The currents were highly coherent (coherence squared > 0.65 , not shown) between 15 and 35 m, i.e., at depths where the flow was almost exclusively directed toward the Sea of Marmara. The currents at deeper depths were, however, quite decoupled with those above 35 m. The coherence decreased rapidly with depth and dropped below 0.25 between lower-layer currents observed above 35 m and below 55 m (yellow line in Figure 12b). Moreover, the currents between 55 m and 92 m were again highly coherent (coherence squared > 0.75 , not shown). There was also an indication that at times, the deep currents co-oscillated with the upper-layer currents (those above 15 m) for frequencies between 0.1 cpd and 0.2 cpd (coherence squared ~ 0.48 ; green line in Figure 12b).

5. Currents Versus Flow Forcing Mechanisms

[24] The upper-layer flow in ocean straits usually reacts swiftly to changing atmospheric forcing, especially to the along-strait wind. In the case of the Dardanelles Strait, upper-layer currents were certainly influenced by variable winds. Figure 13 shows along-and across-strait wind stresses and upper-layer along-strait currents. In the northern Dardanelles, the currents followed along-strait winds very closely (Figure 13a). The across-strait wind stress was about an order of the magnitude smaller than the along-strait stress, and it seemed to be irrelevant except for instances when storms

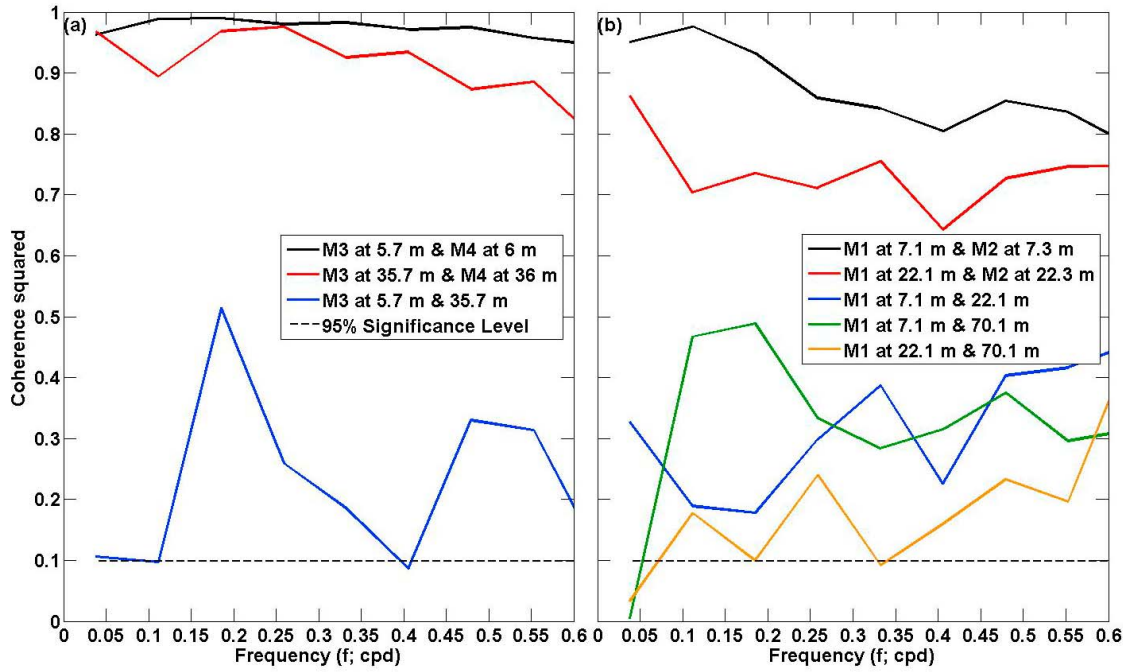


Figure 12. Coherence squared among along-strait currents recorded at various selected depths for (a) the Marmara and (b) Aegean sections; the dashed line is the 95% significance level.

were passing over the TSS. In general, the upper-layer flow was swifter when the along strait wind stress was more negative (toward the Aegean Sea). The flow weakened when this stress became less negative or positive (toward the Sea of Marmara). The upper-layer flow was also blocked and reversed several times. The blockages and reversals of the upper layer were frequent between September 2008 and March 2009, and they were generally associated with passages of cyclones over the TSS region. The longest reversals began on 4 October 2008 and on 21 November 2008, with both lasting longer than 2 days.

[25] In the Aegean section, the upper-layer currents were also impacted by fluctuating wind stresses whose along- and across-strait components were mostly of similar magnitude throughout the deployment (Figure 13b). Note that this change in wind direction with respect to the strait direction is mainly due to a change in the strait direction rather than a change in wind direction between Çanakkale and Bozcaada. The upper-layer flow toward the Aegean Sea again was stronger when both stress components were negative, i.e., when northeasterly winds (toward the southwest) were present over the region. The flow weakened when such wind

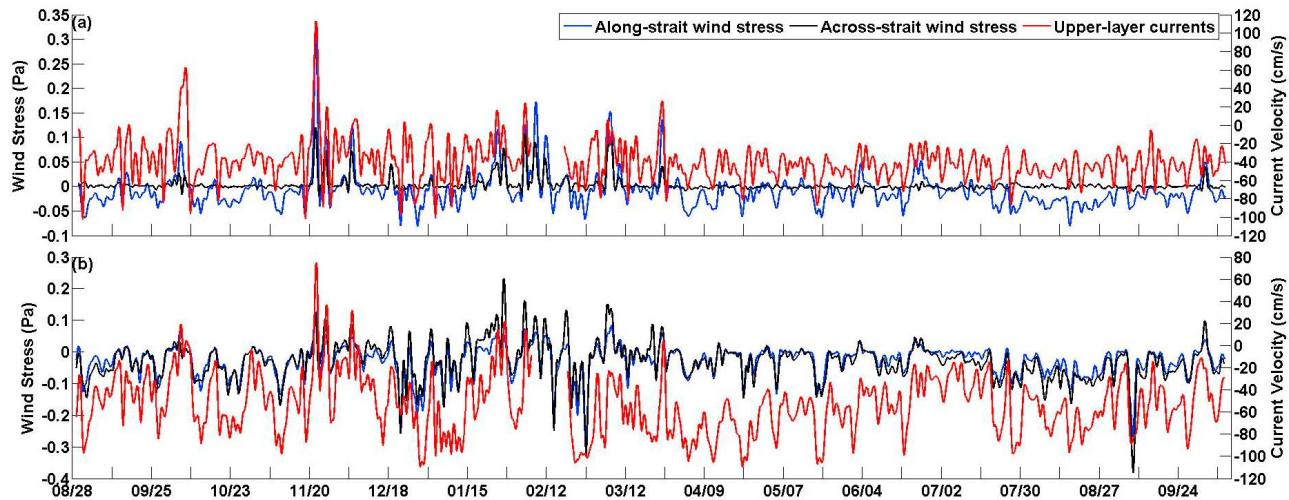


Figure 13. Rotated wind stress components (Pa) and along-strait velocity components (cm/s) in the (a) northern and (b) southern Dardanelles (40-h low-passed data). Wind stress components were estimated from Çanakkale and Bozcaada for the northern and southern sections and rotated 50° and 10°, respectively. Currents (first available depth levels) are from M3 (5.7 m) and M1 (7.1 m) moorings.

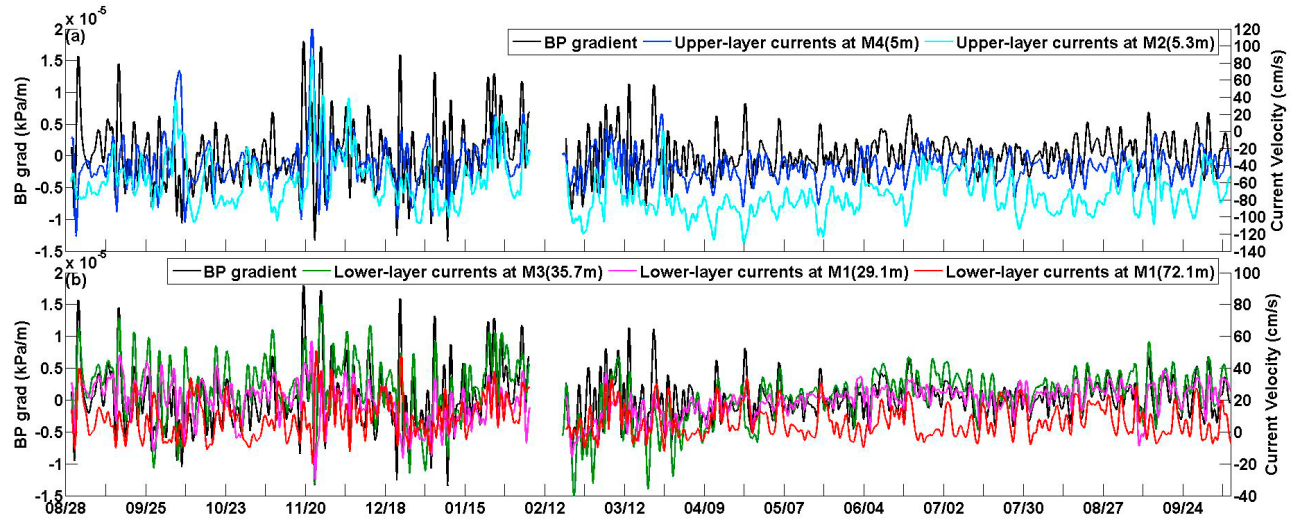


Figure 14. Bottom pressure anomaly gradient (kPa/m) between the southern and northern Dardanelles Strait and (a) upper-layer and (b) lower-layer along-strait currents (cm/s). Upper-layer currents are from M2 (5.3 m) and M4 (5 m) moorings; lower-layer currents are from M1 (29.1 m and 72.1 m) and M3 (35.7 m) moorings; all data are 40-h low-pass.

stress decreased or reversed. Similar to the upper-layer currents in the Marmara section, the upper-layer currents in the Aegean section were blocked and reversed several times and these events occurred when storms were passing over the strait. Current observations indicate that all reversals of the upper-layer flow persisted less than 2 days.

[26] The upper-layer flow was also influenced by BPD variations. Figure 14a shows the upper-layer currents and the bottom pressure (BP) anomaly gradient estimated from the BPD variations divided by the length of the strait (61 km). At both sections, the flow toward the Aegean Sea generally

strengthened when the BP gradient was negative, e.g., one situation that would produce this negative gradient would be for the bottom pressure at the Marmara moorings to be higher than that at the Aegean moorings. Additionally, the atmospheric pressure gradient was one order of magnitude lower than the bottom pressure gradient (Figures 3b and 14a); hence the former contributed little to the BPD and, thereby, little to the observed upper-layer flow variations.

[27] This visual dependence of the flow on atmospheric forcing and the BP anomaly gradient variations is confirmed by results from coherence analyses shown in Figure 15.

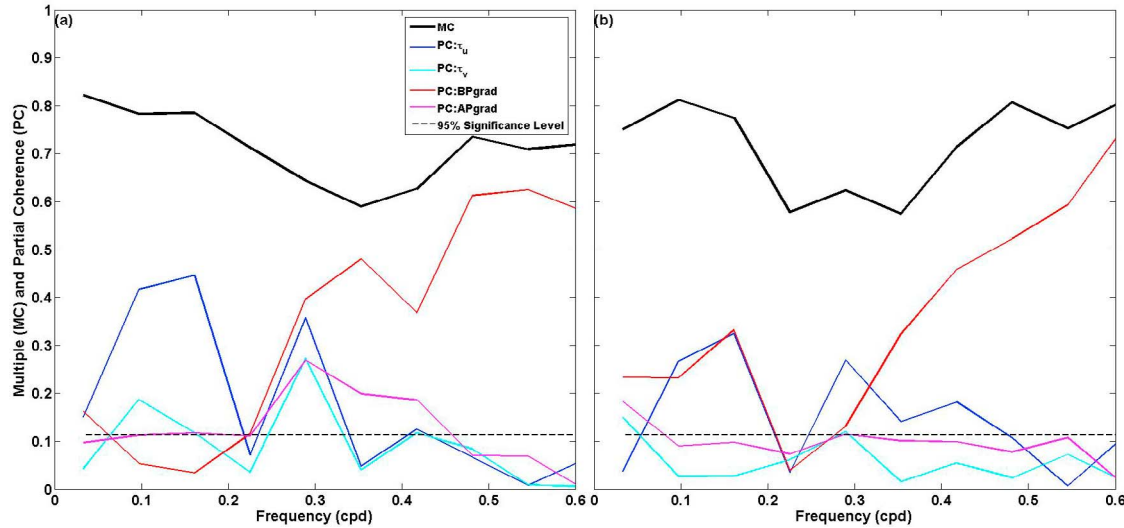


Figure 15. Multiple coherence (MC, black line) and partial coherence (PC, color lines) between the near-surface currents and the bottom pressure anomaly gradient between the southern and northern Dardanelles (red line), the along- (blue line) and across-strait (cyan line) wind stress components, and the atmospheric pressure gradient (magenta line) for (a) the Marmara and (b) Aegean sections; the dashed line is the 95% significance level. Wind stresses calculated from winds collected at Çanakkale and the atmospheric pressure gradient estimated from observations from Bozcaada and Tekirdağ were used in the coherence analyses.

In both sections, the wind stresses, the BP gradient (atmospheric pressure was removed from the BPD), and the atmospheric pressure gradient (atmospheric pressure observations from Tekirdağ and Bozcaada were used to estimate this gradient) are able to explain most, but not all, of the upper-layer flow variability as indicated by the multiple coherence that accounts for 58% to 81% of the current variance in the low-frequency band (<0.6 cpd). Partial coherence results show that the primary forcing mechanisms of the current fluctuations at both sections were the along-strait wind stress and the bottom pressure anomaly gradient. Additionally, the upper-layer currents were also influenced by fluctuations of the across-strait wind stress and the atmospheric pressure gradient with partial coherences above the 95% significance level for some frequencies but their impacts at these frequencies were secondary compared to the along-strait wind stress and the bottom pressure gradient in the northern section. In the Aegean section, partial coherences of the across-strait wind stress and the atmospheric pressure gradient were below the 95% significance level for almost all frequencies indicating their negligible influence on the upper-layer current fluctuations.

[28] To further clarify the role of the along-strait winds and the BP gradient as primary forcings controlling upper-layer flow variability in the Dardanelles Strait, a simple momentum balance for the along-strait current component is employed:

$$\frac{\partial u'}{\partial t} + \frac{r}{h} u' = -g \frac{\partial \eta'}{\partial x} + \frac{\tau_x}{\rho_0 h} \quad (2)$$

where u' is the along-strait current within the upper layer, r is a drag coefficient, h is the thickness of the upper layer, η' is the water level, τ_x is the along-strait wind stress, and ρ_0 is a reference density. Note that u' represents only the flow and its variations that are locally driven solely by winds and water level gradient in the upper layer. Integrating (2) in time and solving for u' yields:

$$u'(t) = \int_0^t \left(-g \frac{\partial \eta'}{\partial x} + \frac{\tau_x}{\rho_0 h} \right) e^{-\frac{r(t-t')}{h}} dt' + u'(t=0) e^{-\frac{rt}{h}} \quad (3)$$

[29] For these computations, the water level gradient term $\left(\frac{\partial \eta}{\partial x}\right)$ was approximated by the demeaned BPD that was first converted to depth variations and then divided by the length of the strait. In addition, atmospheric pressure was also removed from the bottom pressure observations prior to the estimation of the BPD since atmospheric pressure was neglected in equation (2) and was almost identical at the meteorological stations located near both sections (Figure 3a). The approximation for the water level gradient, which is used here, can either overestimate or underestimate the water level gradient mainly due to the fact that the bottom pressure data also include a contribution from the baroclinic pressure anomaly gradient $\left(\frac{\partial \rho}{\partial x}\right)$. This baroclinic gradient fluctuates either positively or negatively as the layer thicknesses change with time. The contribution from this gradient cannot be removed due to limited density observations in the southern Dardanelles Strait. Wind stress was estimated from wind

observations collected at Çanakkale and Bozcaada for the Marmara and Aegean sections, respectively. The friction coefficient (r) was chosen to yield the best agreement with the observations.

[30] Results from the model for the upper-layer currents in the Marmara and Aegean sections are shown in Figure 16. Owing to a 10-day gap in the current and bottom pressure observations, the model results were estimated separately for the first and second part of the deployment. Note that because the model used time anomalies along-strait velocity means had to be added to the final model outputs. For the Marmara section, means of -34 cm/s and -41 cm/s were added to the model results for the first and second part of the deployment, respectively, while means of -41 cm/s and -55 cm/s were added for the Aegean section. Overall, the analytical model results matched the observations better for the Aegean section compared to the Marmara section. Figure 16b shows layer-averaged currents (a mean current was estimated using observations from the first three and the first five depth levels from moorings M1 and M2, respectively) and model output ($h = 10$ m, $r = 0.00025$ m/s, and $\rho_0 = 1022.5$ kg/m³; squared correlation coefficient (R^2) = 0.42). Major events are generally captured by the model driven just by the water level gradient and the along-strait wind stress. Amplitudes of the along-strait current fluctuations, however, are sometimes overestimated.

[31] In the northern section, there are more discrepancies between the mean upper-layer current and the model simulations (Figure 16a; $R^2 = 0.29$, $h = 20$ m, $r = 0.0003$ m/s, and $\rho_0 = 1018$ kg/m³). The mean observed current there was evaluated by averaging measurements recorded at moorings M3 (depths 5.7–15.7 m) and M4 (depths 5–15 m). The model is able to predict fairly well current fluctuations for a few cases despite a generally higher level of disagreement with the observations. The results from the model for both sections are in agreement with the multiple coherence findings indicating that the observed current variability in the upper layer is partly related to the along-strait wind stress and the BP gradient in the Dardanelles Strait.

[32] Fluctuations of the lower-layer flow at both mooring sections were also partially related to variability of the BP gradient (Figure 14b). The flow toward the Sea of Marmara was generally stronger when the BP anomaly gradient was positive. When it decreased and/or became negative the flow in the lower layer usually weakened and often was reversed in the Marmara section (green line in Figure 14b). The dependence of lower-layer current fluctuations on the BP gradient variations was also confirmed by coherence results shown in Figure 17. On average, the BP gradient was able to account for 65% and 63% variance of the lower-layer flow fluctuations with periods ranging between 1.7 days to 10 days in the Marmara and Aegean sections, respectively.

[33] Full reversals of the lower-layer flow in the northern Dardanelles Strait commonly occurred when a strong cyclone passed over the TSS region (Figures 2 and 9). Once a storm reached the TSS region the velocity of the upper-layer flow was usually reduced and often reversed, and based on the salinity time series, vigorous mixing ensued in the northern Dardanelles section (Figure 5a). The bottom pressure observations indicate that the water level can then build up in the Sea of Marmara and decrease in the Aegean Sea resulting in the negative BP anomaly gradient

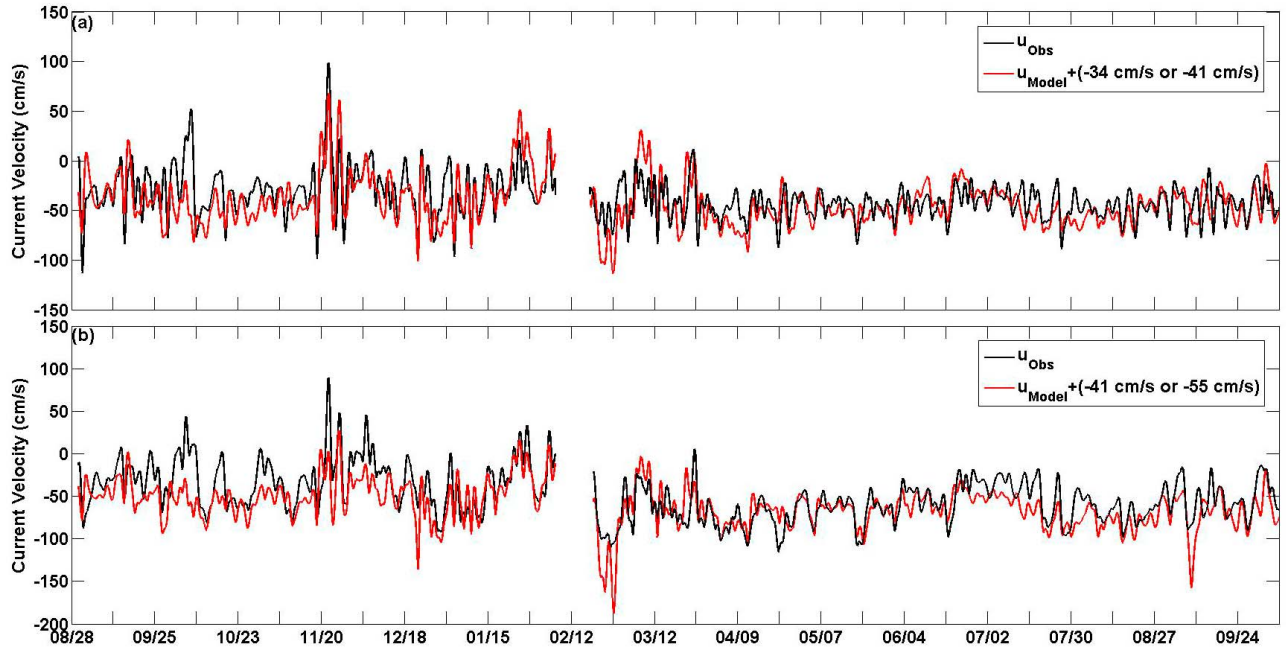


Figure 16. Mean upper-layer along-strait currents (black line) in the (a) Marmara and (b) Aegean mooring sections and currents estimated from the model (equation (2)). Offsets of -34 cm/s and -41 cm/s were added to the model currents for the first and second part of the deployment in the Marmara section, respectively, while offsets were -41 cm/s and -55 cm/s for the Aegean section.

(Figure 14b). Once this gradient was large enough the flow in the lower layer usually reversed for a day or more, as for instance, the reversal that was observed on 6–7 October 2008 after the cyclone impacted the TSS region beginning on 3 October 2008.

[34] Another observed feature of the exchange flow, which seemed to be also related to the wind-forcing and dynamics of the North Aegean Sea, was the deep outflow of high salinity waters flowing to the Aegean Sea as a third layer at the bottom in the southern Dardanelles Strait. Coherence results (not shown) indicate that the wind stress was able to explain from 30% to 56% of the deep outflow variability for fluctuations with periods larger than 3.5 days. What are possible connections between wind-forcing and lower layer dynamics? In the northern part of the Aegean Sea, winds from the northern quadrant, especially northerly and the northeasterly winds prevail and effectively cause strong upwelling along the Turkish east coast [Poulos *et al.*, 1997; Kourafalou and Barbopoulos, 2003; Savvidis *et al.*, 2004; Sayin *et al.*, 2011]. A careful inspection of the concurrent time series of the winds from three meteorological stations and currents from moorings M1 and M2 suggest that the two-layer exchange was generally observed when northerly or northeasterly winds blew over the region. When these winds relaxed and/or switched to southwesterly winds a third deep layer with currents of about 10 cm/s flowing toward the Aegean Sea often developed after a day or so. Winds from the south are downwelling favorable along the Turkish coast in the North Aegean Sea [Kourafalou and Tsiaras, 2007] and are able to increase the sea level toward the coast. This increase in the sea level may change the spatial distribution of the barotropic pressure gradient from those observed during

upwelling as well as alter the baroclinic structure of the Dardanelles Strait outflow plume. Changes in barotropic and baroclinic gradient distributions outside and perhaps inside the southern part of the Dardanelles Strait may lead to a reversal of the flow direction in part of the high-salinity lower

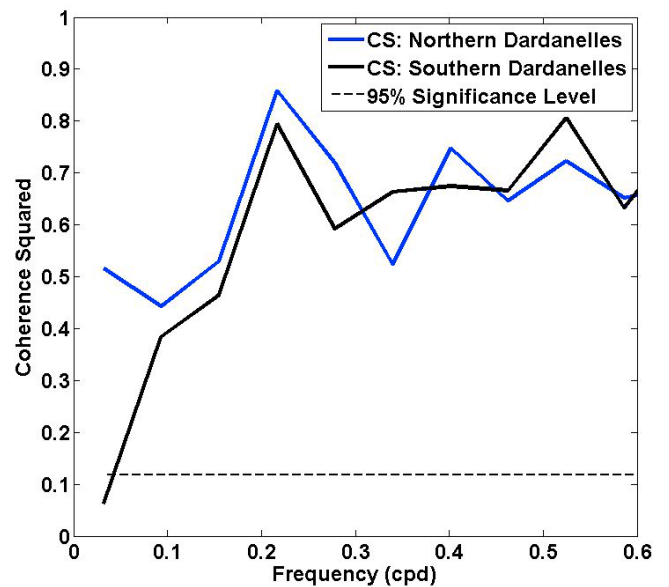


Figure 17. Coherence squared (CS) between along-strait lower-layer currents and the BP anomaly gradient for the northern (blue line, current depth level -40.7 m) and southern (black line, current depth level -30.3 m) mooring sections; the dashed line is the 95% significance level.

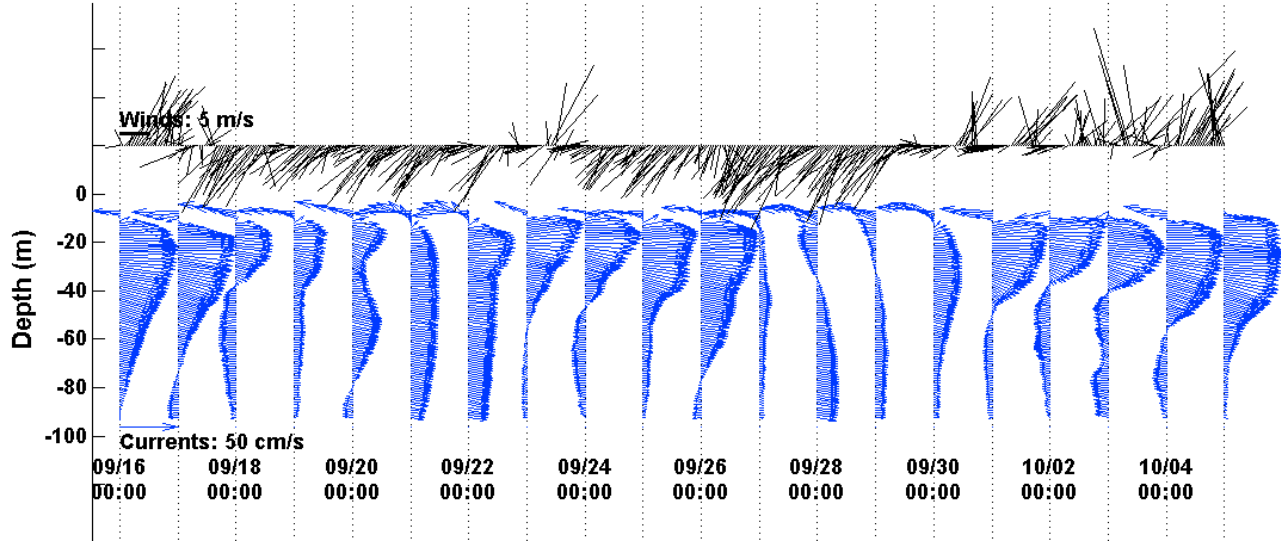


Figure 18. Examples of the three-layer exchange in the southern Dardanelles. Current profiles (blue arrows; cm/s) are from M1 mooring; winds (black sticks; m/s) are from Çanakkale.

layer resulting in an occurrence of the deep outflow to the Aegean Sea. Unfortunately, our data set cannot prove or disprove this hypothesis or show how far inside the strait the third layer could be traced. Additionally, there were also instances when the three-layer exchange occurred briefly during northerly/northeasterly and weak variable winds. Examples of the exchange flow under different wind conditions are shown in Figure 18.

6. Possible Hydraulic Control?

[35] It was indicated by modeling studies of the exchange flow in the Dardanelles Strait that the flow is critical in the Nara Pass region, where the upper layer is supercritical [Oğuz and Sur, 1989; Stashchuk and Hutter, 2001; Kanarska and Maderich, 2008]. Oğuz and Sur [1989] also suggested that this layer may be supercritical near the Aegean exit due to an abrupt expansion of the strait width. The EPOS observations near this exit seem to indicate that this may have been the case for certain times of the deployment, and these instances seemed to occur during strong and persistent northeasterly winds. We used our observations to estimate times series of the composite Froude number for the two-layer exchange flow [Farmer and Armi, 1986]. An approach proposed by Smeed [2000] was also employed since the flow in the southern Dardanelles often consisted of three layers. Owing to limited temperature and salinity data, especially in the upper layer, a constant density for each layer was used, while time series of the layer-averaged along-strait current velocity and layer depths (24-h velocity and depth averages) were utilized for these computations. The following densities were used: $\rho_1 = 1022.5 \text{ kg/m}^3$ and $\rho_2 = 1029.1234 \text{ kg/m}^3$ for the two-layer case. For the three-layer exchange approach, the following values were used: $\rho_1 = 1022.5 \text{ kg/m}^3$, $\rho_2 = 1029.05 \text{ kg/m}^3$, and $\rho_3 = 1029.44 \text{ kg/m}^3$.

[36] Figure 19 shows the time series for the composite Froude number during times of the two-layer exchange flow (black dots) for the Aegean section. For the three-layer exchange, the flow was critical with respect to internal modes

when $\det(M) = h^2 [F_2^4 - (r - F_1^2 - F_2^2)(1 - r - F_2^2 - F_3^2)] = 0$ [Smeed, 2000]. F_i is the Froude number for the i th layer, $r = (\rho_2 - \rho_1)/(\rho_3 - \rho_1)$, and h is the nondimensional depth of the channel. It has been shown by Lane-Serff *et al.* [2000] that at a control the second internal mode is critical if $F_1^2 + F_2^2 < r$, while the first internal mode appears to be critical if $F_1^2 + F_2^2 > r$. Cases of the three-layer exchange flow are also shown in Figure 19 as blue asterisks, while red diamonds indicate times when the determinate is nearly zero ($\det(M) < 10^{-7}$) and the second internal mode is critical, except for 3 April 2009 when the first internal mode appears to be critical. It should be noted that the upper-layer density can vary greatly due to seasonal temperature and salinity changes [Tuğrul *et al.*, 2002] and that the composite Froude number and $\det(M)$ are sensitive to density choices; hence more detailed observations are required to confirm a hydraulic control of the upper layer flow in the southern Dardanelles Strait (near the Aegean exit). Concurrently, the observations in the northern Dardanelles clearly showed that the two-layer exchange flow there was subcritical throughout the entire deployment (composite Froude numbers not shown).

7. Summary and Conclusions

[37] Over the years, the Dardanelles Strait has been less studied and its dynamics less understood than that of the Bosphorus Strait in the TSS region. The Dardanelles Strait is an important component of the TSS because it is the final conduit where brackish waters from the Black Sea are modified before being discharged into the North Aegean Sea. It has been recognized for years that this outflow impacts the surface circulation in this sea [Poulos *et al.*, 1997]. Zervakis *et al.* [2000] have also suggested that in addition to atmospheric conditions, the Dardanelles outflow plays a crucial role in the deep water formation in the North Aegean Sea. The outflow produces a layer with very distinct thickness and hydrographic characteristics (low salinity and low temperature in cold months). As this layer thickens, its impact becomes larger on air-sea fluxes and hence it can act as a

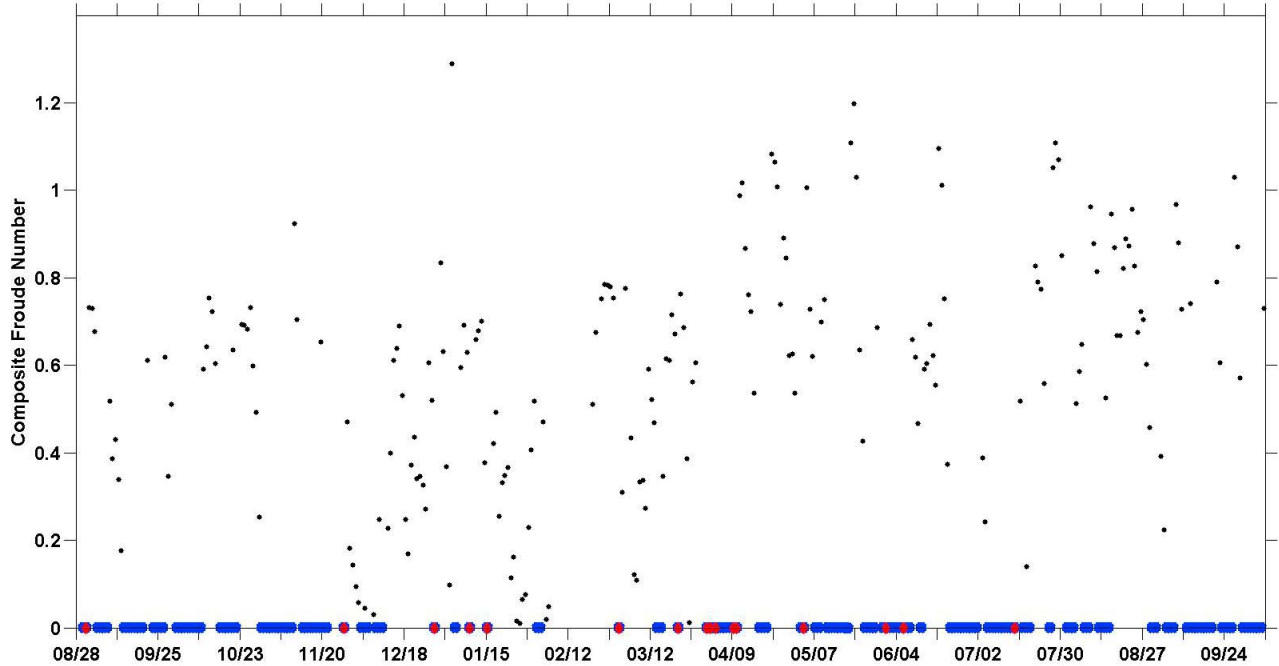


Figure 19. Composite Froude numbers for the two-layer exchange (black dots), times when the three-layer exchange was observed in the Aegean section (blue asterisks), and instances when $\det(M)$ was nearly 0 (red diamonds).

barrier layer preventing underlying denser waters from heat losses during passages of cold atmospheric fronts in winter and subsequently from sinking and contributing to the deep dense water pool in the North Aegean Sea. Moreover, the lower-layer outflow of high salinity waters from the Dardanelles Strait impacts subsurface circulation (below the upper 20–25 m), hydrography, and oxygen distribution in the Sea of Marmara [Beşiktepe *et al.*, 1993, 1994; Beşiktepe, 2003]. This high salinity outflow shows distinct seasonal density variability resulting mainly from seasonal temperature changes. Owing to higher density than the interior of the sea in winter, the outflow attaches to the bottom after leaving the strait, forms a bottom boundary current, and then enters the interior of the sea as a turbulent plume. In fall, the outflow is lighter and manifests itself as a subsurface flow bounded by the upper layer of the Sea of Marmara.

[38] To advance our understanding of the exchange dynamics in the Dardanelles Strait, NRL instituted a field program in the TSS region. As a result of this observational effort, over a yearlong time series of concurrent current and hydrographic observations were collected. The observations proved that the exchange dynamics through the Dardanelles Strait are more complex than previously thought. They showed that on longer timescales (monthly, seasonal, and annual) the basic exchange is a two-layer flow at the mooring locations. There was some seasonal and monthly variability; however, such variability was small in comparison to that observed on shorter timescales (synoptic scale 2–10 days). The upper-layer flow with maximum speeds over 120 cm/s was generally more energetic than that of the lower layer where the currents were below 75 cm/s. It is worth noting that our ADCP moorings did not measure near-surface currents

that were likely even faster. For example, during our initial deployment in August 2008, shipboard current observations indicated near-surface current velocities over 200 cm/s in the Aegean section. Overall, velocity fluctuations of the upper layer flow were more pronounced than those of the flow in the lower layer. The thickness of the upper layer, however, was always much less than that of the lower layer, and it was, on average, about 22 m and 13 m in the Marmara and Aegean sections, respectively. The upper-layer thickness also displayed some variability and was deeper in winter and spring when, for example, it was found to extend to about 32 m and 17 m below the surface in the northern and southern sections, respectively. Because of this limited thickness, the flow in the upper layer was often reduced, stopped, and even reversed by strong winds usually associated with cyclones passing over the TSS region during fall, winter, and spring months. Results from our analyses suggest that variability of the upper-layer flow was coherent with the along-strait wind stress and the bottom pressure anomaly gradient.

[39] Flow fluctuations in the lower layer were of smaller amplitudes than those in the upper layer, and they were highly coherent with the BP gradient variability at both mooring sections on synoptic timescales. Furthermore, the lower layer was at least 40 m thick in the northern Dardanelles, and therefore our observations of it partially or fully reversing usually during or right after a cyclone passage were unexpected. In fact, during most energetic cyclones, the exchange flow was totally reversed for a day or more, i.e., the upper-layer flow moved toward the Sea of Marmara, while the lower-layer currents flowed toward the Aegean Sea. These events were also accompanied by strong mixing and a rise of the bottom pressure (water level) in the Marmara section. This rise

probably led to a buildup of the barotropic pressure gradient that, in turn, was able to reverse the currents in the lower layer.

[40] In the southern Dardanelles Strait (Aegean) section, which is about 100 m deep and about 5 km wide, the exchange flow was asymmetric, i.e., it was sheared horizontally and vertically. The EPOS current observations captured this asymmetry especially well for the lower-layer flow that was stronger at mooring M2 located near the Anatolian coast than at mooring M1 located in the central channel of the strait. The vertical structure of the flow was even more complex when prevailing northeasterly winds, which generate upwelling along the Turkish coast, relaxed or/and switched to winds blowing from the southern quadrant. During these instances, the weak deep salty outflow developed, and the exchange became a three-layer flow with the upper brackish and deep salty layers moving toward the Aegean Sea and the middle (also salty) layer flowing toward the Sea of Marmara. This three-layer exchange lasted briefly, i.e., usually for only a day or two, but sometimes it was observed for as long as a week. Moreover, the EPOS observations seem to indicate that in terms of a two-layer composite Froude number, the upper-layer flow was hydraulically controlled in the southern Dardanelles (near the Aegean exit) on occasion. When the three-layer exchange was present there were also instances when a control was exerted mainly with the second internal mode being critical.

[41] **Acknowledgments.** This work was supported by the Office of Naval Research as a part of the NRL's basic research project "Exchange Processes in Ocean Straits (EPOS)" under Program Element 61153N. We would like to thank everyone from the NATO NURC and the Turkish Navy Office of Navigation, Hydrography, and Oceanography who supported and helped to organize and fund cruises to the TSS on the R/V Alliance. We would like to thank Mark Hulbert, Andy Quaid, Wesley Goode, and Steve Sova, our technicians, for outstanding instrument preparation, mooring deployment, and recovery. We are also thankful and indebted to the crew of the R/V Alliance for helping with our mooring deployment and recovery in very challenging conditions.

References

- Beşiktepe, Ş. T. (2003), Density currents in the two-layer flow: An example of Dardanelles outflow, *Oceanol. Acta*, **26**, 243–253, doi:10.1016/S0399-1784(03)00015-X.
- Beşiktepe, Ş. T., E. Özsoy, and Ü. Ünlüata (1993), Filling of the Marmara Sea by the Dardanelles lower layer inflow, *Deep Sea Res., Part I*, **40**, 1815–1838, doi:10.1016/0967-0637(93)90034-Z.
- Beşiktepe, Ş. T., H. I. Sur, E. Özsoy, M. A. Latif, T. Oğuz, and Ü. Ünlüata (1994), The circulation and hydrography of the Marmara Sea, *Prog. Oceanogr.*, **34**, 285–334, doi:10.1016/0079-6611(94)90018-3.
- Eremeev, V. N., N. M. Stashchuk, V. I. Vlasenko, V. A. Ivanov, and O. Uslu (1999), Some aspects of the water exchange through the Dardanelles Strait, in *The Eastern Mediterranean as a Laboratory Basin for the Assessment of Contrasting Ecosystems*, edited by P. Malanotte-Rizzoli and V. N. Eremeev, pp. 301–312, Kluwer Acad., Norwell, Mass.
- Farmer, D. M., and L. Armi (1986), Maximal two-layer exchange over a sill and through the combination of a sill and contraction with barotropic flow, *J. Fluid Mech.*, **164**, 53–76, doi:10.1017/S002211208600246X.
- Kanarska, Y., and V. Maderich (2003), Non-hydrostatic modeling of exchange flows, paper presented at XXX Congress, Int. Assoc. for Hydro-Environ., Thessaloniki, Greece.
- Kanarska, Y., and V. Maderich (2008), Modelling of seasonal exchange flows through the Dardanelles Strait, *Estuarine Coastal Shelf Sci.*, **79**, 449–458, doi:10.1016/j.ecss.2008.04.019.
- Kasai, A., A. E. Hill, T. Fujiwara, and J. H. Simpson (2000), Effect of the Earth's rotation on the circulation in regions of freshwater influence, *J. Geophys. Res.*, **105**(C7), 16,961–16,969, doi:10.1029/2000JC900058.
- Kourafalou, V. H., and K. Barbopoulos (2003), High resolution simulations on the North Aegean Sea seasonal circulation, *Ann. Geophys.*, **21**, 251–265, doi:10.5194/angeo-21-251-2003.
- Kourafalou, V. H., and K. P. Tsiaras (2007), A nested circulation model for the North Aegean Sea, *Ocean Sci.*, **3**, 1–16, doi:10.5194/os-3-1-2007.
- Lane-Serff, G. F., D. A. Smeed, and C. R. Postlethwaite (2000), Multi-layer hydraulic exchange flows, *J. Fluid Mech.*, **416**, 269–296, doi:10.1017/S002211200008958.
- Oğuz, T., and H. I. Sur (1989), A two-layer model of water exchange through the Dardanelles Strait, *Oceanol. Acta*, **12**, 23–31.
- Perkins, H., F. de Strobel, and L. Gualdesi (2000), The Barny Sentinel Trawl-resistant ADCP bottom mount: Design, testing, and application, *IEEE J. Oceanic Eng.*, **25**, 430–436, doi:10.1109/48.895350.
- Poulos, S. E., P. G. Drakopoulos, and M. B. Collins (1997), Seasonal variability in sea surface oceanographic conditions in the Aegean Sea (Eastern Mediterranean): An overview, *J. Mar. Syst.*, **13**, 225–244, doi:10.1016/S0924-7963(96)00113-3.
- Savvidis, Y. G., M. G. Dodou, Y. N. Krestenitis, and C. G. Koutitas (2004), Modeling of the upwelling hydrodynamics in the Aegean Sea, *Mediterr. Mar. Sci.*, **5**(1), 5–18.
- Sayin, E., C. Eronat, Ş. Uçkaç, and Ş. T. Beşiktepe (2011), Hydrography of the eastern part of the Aegean Sea during the Eastern Mediterranean Transient (EMT), *J. Mar. Syst.*, **88**, 502–515, doi:10.1016/j.jmarsys.2011.06.005.
- Smeed, D. A. (2000), Hydraulic control of three-layer exchange flows: Application to the Bab al Mandab, *J. Phys. Oceanogr.*, **30**, 2574–2588, doi:10.1175/1520-0485(2000)030<2574:HCOTLE>2.0.CO;2.
- Stashchuk, N., and K. Hutter (2001), Modelling of waters exchange through the Strait of the Dardanelles, *Cont. Shelf Res.*, **21**, 1361–1382, doi:10.1016/S0278-4343(01)00017-6.
- Tuğrul, S., Ş. T. Beşiktepe, and İ. Salihoglu (2002), Nutrient exchange fluxes between the Aegean and Black Seas through the Marmara Sea, *Mediterr. Mar. Sci.*, **3**(1), 33–42.
- Ünlüata, Ü., T. Oğuz, M. A. Latif, and E. Özsoy (1990), On the physical oceanography of the Turkish Straits, in *The Physical Oceanography of Sea Straits*, edited by L. J. Pratt, pp. 25–60, Kluwer Acad., Dordrecht, Netherlands.
- Valle-Levinson, A. (2008), Density-driven exchange flow in terms of the Kelvin and Ekman numbers, *J. Geophys. Res.*, **113**, C04001, doi:10.1029/2007JC004144.
- Valle-Levinson, A., C. Reyes, and R. Sanay (2003), Effects of bathymetry, friction and Earth's rotation on estuary/ocean exchange, *J. Phys. Oceanogr.*, **33**(11), 2375–2393, doi:10.1175/1520-0485(2003)033<2375:EOBFAR>2.0.CO;2.
- Zervakis, V., D. Georgopoulos, and P. G. Drakopoulos (2000), The role of the North Aegean in triggering the recent Eastern Mediterranean climatic changes, *J. Geophys. Res.*, **105**, 26,103–26,116, doi:10.1029/2000JC900131.